Received: 31 August 2022 | Revised: 22 January 2023 | Accepted: 25 January 2023
DOI: 10.1002/hipo.23513

REVIEW

WILEY

Gated transformations from egocentric to allocentric reference frames involving retrosplenial cortex, entorhinal cortex, and hippocampus

Andrew S. Alexander | **Jennifer C. Robinson** | **Chantal E. Stern** | **Michael E. Hasselmo**

Center for Systems Neuroscience, Boston University, Boston, Massachusetts, USA

Correspondence
Andrew S. Alexander, Jennifer C. Robinson, and Michael E. Hasselmo, Center for Systems Neuroscience, Boston University, 610 Commonwealth Avenue, Boston, MA 02215, USA.
Email: asalexan@gmail.com, jenniferclaire.robinson@gmail.com, and hasselmo@bu.edu

Funding information
National Institute of Mental Health, Grant/Award Numbers: R01 MH060013, R01 MH120073; National Institute of Neurological Disorders and Stroke, Grant/Award Number: F32 NS101836; Office of Naval Research, Grant/Award Numbers: DURIP N00014-17-1-2304, MURI N00014-16-1-2832, MURI N00014-19-1-2571

Abstract

This paper reviews the recent experimental finding that neurons in behaving rodents show egocentric coding of the environment in a number of structures associated with the hippocampus. Many animals generating behavior on the basis of sensory input must deal with the transformation of coordinates from the egocentric position of sensory input relative to the animal, into an allocentric framework concerning the position of multiple goals and objects relative to each other in the environment. Neurons in retrosplenial cortex show egocentric coding of the position of boundaries in relation to an animal. These neuronal responses are discussed in relation to existing models of the transformation from egocentric to allocentric coordinates using gain fields and a new model proposing transformations of phase coding that differ from current models. The same type of transformations could allow hierarchical representations of complex scenes. The responses in rodents are also discussed in comparison to work on coordinate transformations in humans and non-human primates.

KEYWORDS
coordinate transformation, population coding, problem solving, spatial navigation, theta oscillations

1 | INTRODUCTION AND REVIEW OF EXPERIMENTAL DATA

Recent electrophysiological recordings in rodents have demonstrated that neurons can code environmental barriers and objects in egocentric coordinates. Here, egocentric coordinates are defined as coordinates reflecting the position of features relative to the animal's sensory input organs. Data demonstrates neurons that generate spikes based on the distance and angle relative to the animal of the barrier or other features. These egocentric boundary cells have been found in multiple structures including the retrosplenial cortex (Alexander et al., 2020; van Wijngaarden et al., 2020), the postrhinal cortex (Gofman et al., 2019; LaChance et al., 2019), the entorhinal cortex (Wang et al., 2018; Wang et al., 2020), and dorsomedial striatum (Hinman et al., 2019).

These neuronal responses based on egocentric coordinates may be essential to important cognitive processes including the facilitation of transformations of sensory input from egocentric coordinates (Figure 1b) to allocentric coordinates (Figure 1c) for goal directed behavior. As shown in Figure 1a, visual sensory inputs arrive in the retinotopic coordinate frame. This is transformed into a head or body-centered egocentric coordinate frame. The egocentric coordinate frame maps the position of barriers and objects relative to the animal (Figure 1b). These egocentric representations may be important for the formation of neural representations coding awareness of the animal's location in allocentric coordinates. The allocentric representation (Figure 1c) codes the position of barriers, objects, and the animal's

---

Andrew S. Alexander and Jennifer C. Robinson are co-first authors.

Special Issue on Hippocampal system neurons encoding views in different species.

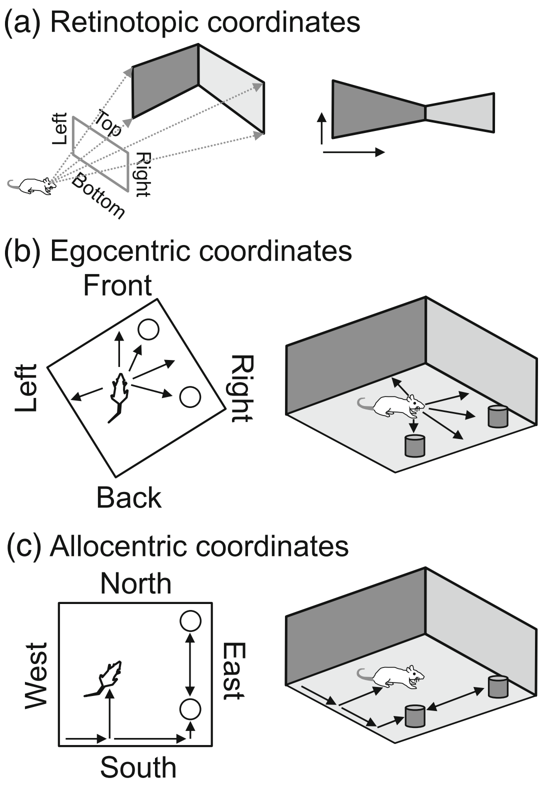

FIGURE 1 Schematic overview of egocentric versus allocentric coordinates. (a) Animals receive and detect sensory input in coordinates centered around specific receptor organs. For example, visual input arrives in retinotopic coordinates as shown on the right. (b) Egocentric coordinates. The sensory input about an environment barrier or object may be coded initially in egocentric coordinates (front, back, left right), based on the angle and distance relative to the animal (arrows). (c) Allocentric coordinates. The same scene can be considered in allocentric coordinates, concerning the location of the animal relative to barriers and objects. Arrows indicate coordinates of the position of the animal and objects relative to environmental barriers, rather than relative to the animal (Bicanski & Burgess, 2018; Byrne et al., 2007; Raudies & Hasselmo, 2015).

own position relative to other features in the environment, such as the position of defining landmarks in the environment, including those not currently seen. The role of the hippocampal formation in these transformations has been discussed in many theoretical papers (Burgess et al., 2001; Recce & Harris, 1996). The transformation from egocentric to allocentric coordinates is important for the process of planning new routes during spatial navigation. If an animal wishes to find its way from an arbitrary starting location to a previously visited but currently unseen goal location, it needs the awareness of its allocentric position in the environment to generate actions to find the goal location.

This paper will start by reviewing data on the coding of boundaries in egocentric coordinates, and discuss this in relationship to models of the coding of boundaries in allocentric coordinates. The discussion will then address how the coding of boundaries in egocentric and allocentric coordinates relates to the coding of the animal's position in allocentric coordinates by grid cells in entorhinal cortex and place cells in the hippocampus. We will examine how these neuronal responses relate to the coding of spatial views in humans and nonhuman primates. Finally, the transformation between coordinate frames will be discussed in the context of prior models and new models.

The question of transformation between coordinates arises in many cognitive processes. This includes the perception of self-location in the environment based on both tracking of self-motion and the sensory experience of externally anchored landmarks. Beyond navigation, transformations are also required for integrating egocentric views of an object or pattern to form allocentric or object-centered representations of the object or pattern needed for recognition, movement planning, and problem solving. These processes all involve some transformation from sensory input in egocentric coordinates to a stable representation in semantic or episodic memory that can be used to build complex hierarchical representations of the environment and objects. Recognizing an object could require transformation from a specific egocentric viewpoint of the object to some internal stored allocentric representation of the relationship between the features of the object (Bicanski & Burgess, 2019; Lewis et al., 2019). Similarly, recognizing a specific environment is like recognizing an object from the inside, requiring matching of a specific configuration of features to the configuration in a memory of a specific object or environment. Understanding the process of coordinate transformations could be relevant to fascinating questions about how cortical circuits form representations of a broad range of objects and environments for the planning of future behavior, even in complex reasoning tasks such as Raven's progressive matrices (Raven, 2000) or the Abstraction and Reasoning Challenge (ARC; Chollet, 2019). In particular, these reasoning tasks require observation of a specific egocentric configuration of sensory features and matching this to a stored representation that allows coding of allocentric relationships between features (Bicanski & Burgess, 2018; Do & Hasselmo, 2021; Kunda et al., 2013; Rasmussen & Eliasmith, 2014; Raudies & Hasselmo, 2017). The relationships between features can then be represented by transformation of coordinates in spatial dimensions such as rotation, size and translation known as affine transformations, but could also extend to features such as systematic changes based on color and shape.

1.1 | Egocentric boundary cells in rodents

As mentioned above, several recent studies have described egocentric boundary cells in a variety of structures associated with the hippocampal formation, including the retrosplenial cortex (Alexander et al., 2020; van Wijngaarden et al., 2020), the postrhinal cortex (Gofman et al., 2019; LaChance et al., 2019), and the entorhinal cortex (Wang et al., 2018; Wang et al., 2020) as well as structures receiving output from these regions such as the dorsomedial striatum (Hinman et al., 2019) and parietal cortex (Alexander et al., 2020). These cells appear consistent with earlier descriptions of direction-dependent place cells (Cho & Sharp, 2001). Figure 2 shows a summary of some of these anatomical structures in rodent brain that contain neurons that show egocentric boundary responses and their relationship to the hippocampus. The figure also gives an overview of some of the other functional cell types and their potential interactions.

As an overview of the phenomenon of egocentric boundary cells, Figure 3 shows the responses of egocentric boundary cells recorded in the retrosplenial cortex (Alexander et al., 2020). Figure 3a1 shows a plot in allocentric coordinates that depicts the allocentric position of the animal relative to the environment at the time of each spike fired by a single egocentric boundary cell (Alexander et al., 2020). The trajectory of the animal as it forages for scattered bits of cereal is shown with the gray line. Each time a spike occurs, the position of the animal is plotted as a colored point. The color of the point indicates the current head direction of the animal shown by the color wheel (i.e., pink = northeast). The large pink circle (surrounded by a blue circle) highlights the position of the animal at the time of a single spike. The head direction of the animal is shown for this example spike (black line vector with arrow) and the straight black lines radiating from the large pink circle show measurement of the distance and angle to each wall from the rat's position at the time of the spike. The figure shows a subsample of angles, whereas in analysis of data, 360 degrees of angle are sampled.

Figure 3a2 shows data for the same spike at the large pink circle in Figure 3a1, but plotted in egocentric coordinates with the rat at the center (Alexander et al., 2020). The thick blue and gray lines show the position of the arena walls in egocentric coordinates, and the thick blue line indicates where the arena walls exist within 62.5 cm of the animal (62.5 cm is a length equivalent to half the length of the arena sides for this experiment). The black lines at different angles show the distance to the barrier plotted in egocentric coordinates in Figure 3a2, matching the lines in allocentric coordinates in Figure 3a1.

(a) Anatomical structures

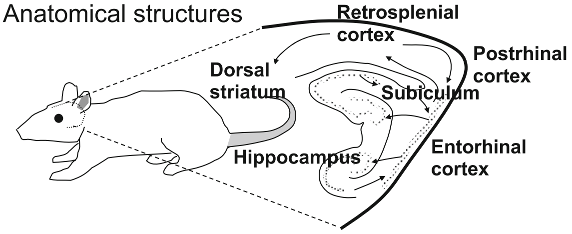

(b) Functional interactions

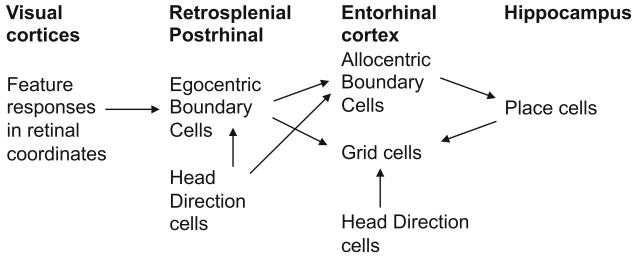

FIGURE 2 (a) Schematic representation of the rodent anatomy showing the location of the retrosplenial cortex and postrhinal cortex with bidirectional connections with the entorhinal cortex, which has bidirectional connections with the hippocampus. The medial septum provides cholinergic, GABAergic and glutamatergic innervation of the entorhinal cortex and of the hippocampus via the fornix. (b) Potential functional interactions are shown. Visual cortex areas on the dorsal surface project to both retrosplenial cortex and postrhinal cortex, both of which contain egocentric boundary cells and head direction cells. Both retrosplenial and postrhinal cortex project to entorhinal cortex. The interaction of egocentric boundary cells and head direction cells is proposed to generate allocentric boundary cells (Bicanski & Burgess, 2018; Byrne et al., 2007) and grid cells. Allocentric boundary cells can generate place cells, which can drive grid cells. Grid cells are proposed to provide affine transformations between egocentric input and different place cell codes.

Figure 3a3 shows the different position of the barriers for three different spikes in egocentric coordinates for each spike, and Figure 3a4 shows the firing rate for all possible barrier positions (Alexander et al., 2020). This shows that this neuron is tuned for specific egocentric positions of barriers to the front and left of the animal. Neurons with this form of receptive field are active whenever any environmental boundary occupies a specific range of angles and distances relative to the animal itself. Across the population of neurons, peak firing rate responses occur when the boundary is at a range of different distances from the animal (Figure 3b) and at a range of specific angles relative to angle zero defined in front of the animal (Figure 3c). The functional need is not clear for the bias toward left and right side lateral responses but might result from the lateral placement of rodent eyes.

The finding of egocentric boundary cells in retrosplenial cortex is exciting for supporting models proposing that retrosplenial cortex mediates transformation of representations of boundaries from egocentric coordinates to allocentric coordinates (Bicanski & Burgess, 2018; Byrne et al., 2007). Models of this transformation will be reviewed in a later section of this review. The finding of egocentric boundary cells supports a wide range of previous work in retrosplenial cortex supporting its role in spatial navigation and awareness of self-location. Neurons in retrosplenial cortex had previously been shown to respond to positions along a route (Alexander & Nitz, 2015, 2017; Mao et al., 2017, 2018, 2020). Earlier research showed that some retrosplenial neurons also respond to the head direction of the animal (Chen, Lin, Barnes, & McNaughton, 1994; Chen, Lin, Green, et al., 1994), and this has been supported by many subsequent studies (Alexander et al., 2020; Cho & Sharp, 2001; Jacob et al., 2017; Voigts & Harnett, 2020).

Egocentric boundary cells have been described in a range of other regions, including areas of dorsomedial striatum (Hinman et al., 2019) receiving input from the retrosplenial and medial entorhinal cortices, where egocentric boundary cells responded to barrier angles primarily lateral to the animal's nose (though some coded positions directly in front or behind the animal) and distances concentrated within specific ranges (approximately 6, 13, and 26 cm). The concentration at specific preferred distances could indicate the spatial resolution for associating navigational goals with the execution of specific action sequences such as whisking at short range versus full body movement on longer scales. Egocentric boundary

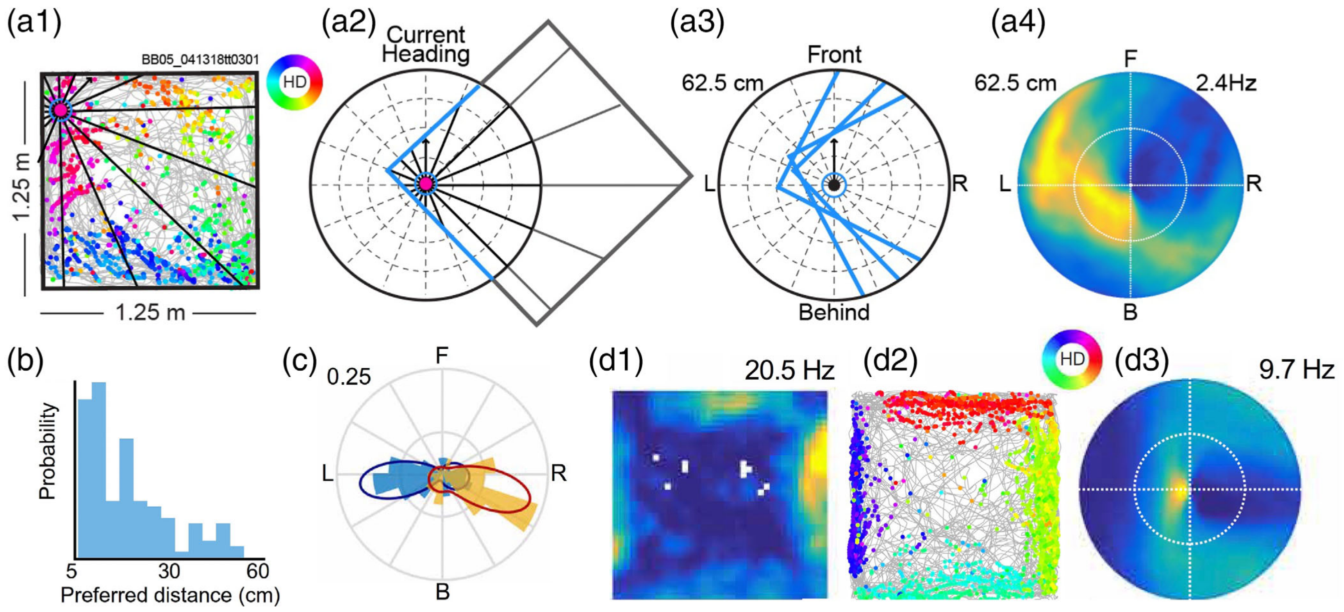

FIGURE 3 Responses of an egocentric boundary cell in retrosplenial cortex. (a1) Plot in allocentric coordinates shows foraging trajectory in gray. Each time a spike occurs, animal position is plotted as a point with color indicating head direction (color wheel indicates directional coding). (a2) Boundaries within 62.5 cm of animal (blue) are plotted in egocentric coordinates relative to animal head direction for a single spike. (a3) Boundary positions for three spikes. (a4) Example egocentric boundary ratemap constructed after repeating steps A1–A3 for all spikes and normalizing by occupation. Color axis indicates zero (blue) to peak firing (yellow) for this neuron (using MATLAB Parula colormap). (b) Probability distribution of preferred distance from boundary of all retrosplenial cortex egocentric boundary cells. (c) Polar histograms and probability density estimates of preferred boundary bearing of all retrosplenial cortex EBCs. Yellow and blue bars correspond to EBCs recorded in the left and right hemisphere, respectively. (d) Another example EBC recorded in the retrosplenial cortex. (d1) Two-dimensional ratemap shows firing rate for animal position in 1.25 m^2 square environment (blue is no firing, yellow is peak firing rate). (d2) Plot of trajectory in gray with color of dot indicating head direction of animal at time of spike. (d3) Egocentric plot showing receptive field on the left side of the animal. *Adapted from* Alexander et al., 2020

vector responses in dorsal striatum are invariant to the visual pattern on environmental boundaries indicating some insensitivity to high-level visual features (Hinman et al., 2019). Another early published report observed neurons in the lateral entorhinal cortex that responded at particular egocentric bearings to boundaries, objects, and goal locations (Wang et al., 2018). This and other evidence for egocentric coding of environments has been reviewed (Bicanski & Burgess, 2020; Wang et al., 2020).

Egocentric boundary cells also appear in other cortical regions, including postrhinal cortex (Gofman et al., 2019; LaChance et al., 2019) as well as secondary motor cortex (Alexander et al., 2020; Gofman et al., 2019). Egocentric boundary cells continue to fire to barriers in darkness in postrhinal cortex (LaChance et al., 2019) and retrosplenial cortex (van Wijngaarden et al., 2020) and to barriers behind the animal (Alexander et al., 2020), supporting a role of memory for barrier position based on prior contact with the barrier. In the postrhinal cortex and entorhinal cortex, egocentric responses appear to be anchored to points in the center of the environment (LaChance et al., 2019; Wang et al., 2018). In a stable symmetrical environment, points in the center of an environment maintain a constant vector to boundary positions, making it difficult to statistically distinguish tuning to center points from tuning to points on the barrier wall. Some experiments in which the size of the environment was expanded show that the response to barriers occurred at the same egocentric distance, suggesting a response to the barriers and not center points (Alexander et al., 2020; Hinman et al., 2019). The detection of boundaries might be a precursor to the detection of the center of an environment that requires experience of the relative relationships between barrier walls (LaChance & Taube, 2022).

Egocentric boundary cells have also been demonstrated in the parietal cortex (Alexander et al., 2020). A wide range of studies have implicated the parietal cortex in the egocentric coding of the environment and planned actions. Recordings in rodents have shown parietal neurons responsive to the upcoming direction and distance of a specific movement in the environment (Nitz, 2006; Nitz, 2009; Nitz, 2012; Whitlock et al., 2008; Whitlock et al., 2012), as well as the egocentric direction to a visual cue (Alexander et al., 2022; Wilber et al., 2014). These rodent studies build on a long history of recordings in parietal cortex of non-human primates showing responses of neurons to the egocentric position of a visual cue or the target of a future movement (Georgopoulos, 1987; Kalaska et al., 1983; Mountcastle et al., 1975).

In summary, a variety of neurophysiological studies show encoding of environmental features such as arena walls, boundaries and objects in egocentric coordinates that depend upon the direction and distance relative to the animal.

1.2 | Phase coding of coordinates

The representation of spatial dimensions could involve different methods of coding, with primary candidates including coding by mean firing rate or temporal coding by phase of spiking. Neuronal spiking activity in the hippocampus and entorhinal cortex shows robust phase coding relative to theta rhythm oscillations in the local field potential (Hafting et al., 2008; O'Keefe & Recce, 1993). Theta rhythm refers to large amplitude oscillations at 4–12 Hz in the field potential of hippocampus and entorhinal cortex associated with the synchrony of synaptic activity in these regions (Buzsaki, 2002). Theta phase-specific activation may play an important role in coding of information. Experimental data on recordings of evoked synaptic potentials in slice preparations and in vivo preparations has shown that the phase of synaptic activation relative to theta is associated with potentiation or depotentiation of synapses between neural populations (Hyman et al., 2003; Orr et al., 2001; Pavlides et al., 1988). Based on this data on potentiation as well as systematic changes in strength of different pathways, the theta phase of synaptic activity is proposed to underlie encoding versus retrieval of processed information including memories (Hasselmo et al., 2002). Differences in phase of firing for encoding versus retrieval dynamics is supported by experimental work in multiple structures (Douchamps et al., 2013; Manns et al., 2007; Poulter et al., 2021; Siegle & Wilson, 2014; Wells et al., 2013). Here, the discussion will focus on the potential role of theta phase in coding spatial information, with less emphasis on the shift between encoding and retrieval dynamics, though the two mechanisms have been modeled together (Hasselmo & Eichenbaum, 2005).

Evidence for phase coding of spatial information in behaving animals includes both phase locking (Fox et al., 1986) and theta phase precession to spatial location in hippocampus (O'Keefe & Recce, 1993; Skaggs et al., 1996). In theta phase precession, a neuron starts out spiking at late phases of theta as an animal enters the firing field of a neuron, and progressively shifts to earlier phases of theta as the animal progresses through the firing field (O'Keefe & Recce, 1993; Skaggs et al., 1996). Entorhinal neurons also show both theta phase locking (Deshmukh et al., 2010; Jeffery et al., 1995; Newman & Hasselmo, 2014) and phase precession to spatial location (Climer et al., 2013; Hafting et al., 2008; Jeewajee et al., 2014). This raises the interesting question of the role of phase coding for egocentric and allocentric representations in structures such as retrosplenial cortex. Phase coding could also influence the coordination of ripples during consolidation of memories (Nitzan et al., 2020).

Local field potentials in retrosplenial cortex show robust theta rhythmicity correlated with hippocampal theta rhythmicity (Alexander et al., 2018; Koike et al., 2017), and some retrosplenial cortex egocentric boundary cells exhibit theta phase locking (Alexander et al., 2020). Phase locking could represent properties of the sensory input. Phase locking could also allow different phases for perception of sensory input and comparison with previously memorized information as proposed for separate phases of encoding and retrieval in the hippocampus (Hasselmo et al., 2002), and as a component of other models involving perception and comparison with memory (Rao & Ballard, 1999). In fact, allocentric boundary cells in the subiculum fire on one phase of theta during experience of a novel inserted boundary, whereas they fire on a different phase when responding to a familiar boundary or firing on the basis of the memory of boundaries that are no longer present (Poulter et al., 2019; Poulter et al., 2021). This study on allocentric coding of boundaries raises the important question of the relationship between egocentric coding and allocentric coding of boundaries.

1.3 | Relation to allocentric boundary cells

The discovery of egocentric coding of boundaries was preceded many years earlier by the prediction (Hartley et al., 2000; O'Keefe & Burgess, 1996) and experimental discovery (Barry et al., 2006; Lever et al., 2009; Poulter et al., 2021; Savelli et al., 2008; Solstad et al., 2008) of allocentric coding of boundaries. At first glance, the egocentric and allocentric coding of boundaries responses might initially appear similar, and there might in fact be neurons that show mixed selectivity that combines these responses. However, the definition of an egocentric boundary response is dependent on the directional relationship of the boundary to the animal's current head direction. Thus, as shown in Figure 3, egocentric responses will appear for all four walls with different head directions (Alexander et al., 2020). In contrast to the egocentric directional relationship of boundary to animal, the allocentric boundary response depends on the allocentric directional relationship of the animal to the boundary in terms of compass direction in the environment (Barry et al., 2006; Burgess & O'Keefe, 1996; Lever et al., 2009; Poulter et al., 2021). So allocentric boundary cells will tend to respond to a subset of one or two barriers in an environment when the animal is at a particular allocentric compass direction and distance relative to the barrier.

The prediction of allocentric boundary cells arose from the influence of shifting barrier walls (to expand or contract an environment) on the firing of place cells (O'Keefe & Burgess, 1996). In particular, the stretching or splitting of cells with expansion led to the hypothesis that place cells are driven by “boundary vector cells” that code the allocentric angle and distance of an animal relative to a boundary (Burgess et al., 2000; Hartley et al., 2000; Hartley et al., 2014; Savelli et al., 2008). This contrasts with the egocentric boundary cells described above that respond to the egocentric angle and distance of boundary relative to an animal. Many years after the initial insightful prediction of allocentric boundary vector cells, this proposal was supported by the experimental discovery of neurons that fired when an animal was at a specific allocentric angle and distance from boundaries (Barry et al., 2006; Lever et al., 2009; Savelli et al., 2008; Solstad et al., 2008). This appears as a neuron firing when an animal is close to boundaries in one compass direction (i.e. when the animal is to the North of a boundary). These allocentric boundary responses can occur well out of whisker range from a boundary (Lever et al., 2009), and can be evoked by boundaries consisting of both wall barriers and the drop off at the edge of a table (Lever et al., 2009; Stewart et al., 2014). Similarly, many egocentric boundary cells do not change their firing when the visual pattern on the walls is altered (Hinman et al., 2019), and many of them continue to fire in darkness (LaChance et al., 2019; van Wijngaarden et al., 2020), or when a boundary wall is replaced by a drop-off (van Wijngaarden et al., 2020). However, other cells do change their response when the wall is replaced by a drop-off (Alexander et al., 2020). Related neurons termed object vector cells respond when an animal is at specific allocentric angles and distances from non-boundary landmarks in lateral entorhinal cortex (Deshmukh & Knierim, 2011) and the hippocampus (Deshmukh & Knierim, 2013) and in medial entorhinal cortex (Hoydal et al., 2019). Both allocentric and egocentric object vector cells were modeled in network simulations (Bicanski & Burgess, 2018).

The same modeling framework that predicted the existence of allocentric boundary cells on the basis of changes in place cell firing cells (Burgess et al., 2000; Hartley et al., 2000) was extended to predict that the generation of allocentric boundary cells could depend upon head direction input combined with egocentric coding of environment boundaries (Bicanski & Burgess, 2018; Burgess et al., 2001; Byrne et al., 2007), thereby predicting the later discovery of egocentric boundary cells. Thus, these models focus on a progression that starts with a transformation from egocentric boundary cells that are combined with head direction coding to form the representation of allocentric boundary cells. Following this, the models (Bicanski & Burgess, 2018; Byrne et al., 2007) propose that the allocentric representation of boundaries could be combined to code allocentric spatial location. Thus, this modeling work can account for the change in spatial firing location of place cells with the movement of environment walls such as expansion or contraction (O'Keefe & Burgess, 1996). An interesting additional question concerns the mechanism for the change in the position and spacing of grid cell firing fields caused by the movements of the environment walls (Barry et al., 2007; Munn et al., 2020; Stensola et al., 2012), which is influenced by knockout of a membrane current known as h current which also affects the coding of velocity in entorhinal cortex (Munn et al., 2020). The response of grid cells to barrier movement has been modeled based on selective influences of the angle and optic flow of visual cues from different parts of the visual field (Raudies & Hasselmo, 2015; Sherrill et al., 2015). Another interesting question concerns the role of phase of firing relative to theta rhythm. Allocentric boundary cells in the subiculum show phase specificity relative to theta rhythm oscillations, firing at one phase of theta when an animal initially encounters a novel inserted wall, but firing at a different phase when the cell shows a trace response, firing on the basis of the memory of boundaries that are no longer present (Poulter et al., 2019, 2021).

In summary, the data on egocentric coding of arena walls and boundaries has important links to earlier work showing allocentric coding of arena walls, boundaries, and objects, suggesting that egocentric coordinates are transformed into allocentric coordinates for coding the environment.

1.4 | Allocentric coding of spatial location by grid cells

In addition to the allocentric coding of boundaries observed in entorhinal cortex and subiculum there is extensive evidence for additional allocentric coding of the animal's spatial location. In entorhinal cortex, grid cells provide a distinctive form of location coding. In a rodent foraging in an open field environment, grid cells fire as the animal visits an array of spatial locations that fall on the vertices of tightly packed equilateral triangles (Hafting et al., 2005). Grid cells in dorsal positions within entorhinal cortex fire with a spacing of about 30–40 cm between the centers of the firing fields, and the spacing and size of firing fields increases in a quantal manner in more ventral locations (Barry et al., 2007; Heys et al., 2014; Sargolini et al., 2006; Stensola et al., 2012). Many grid cells fire based on both the current location and the current head direction of the animal (Sargolini et al., 2006), and could therefore mediate both translation and rotation transformations. Neurons in medial entorhinal cortex also show other types of mixed selectivity, and can show spatial selectivity without showing grid cell firing patterns (Diehl et al., 2017; Hardcastle et al., 2017).

As noted above, egocentric boundary cells in retrosplenial and allocentric boundary cells in subiculum do show phase specificity relative to theta rhythm oscillations, but this has not yet been shown to vary systematically for a specific sensory dimension (Alexander et al., 2020). Similarly, grid cells in layer II of entorhinal cortex show strong phase locking to theta that does not vary with position. In contrast, grid cells in layer III and V of entorhinal cortex exhibit robust temporal phase coding of spatial location, in which neurons show phase precession, shifting from spiking at late phases to early phases of theta as an animal runs through the neuron's firing field on a linear track (Hafting et al., 2008), or in an open field (Climer et al., 2013; Jeewajee et al., 2014). Consistent with this precession data, the rhythmicity of entorhinal spiking activity measured by an autocorrelogram shows a slightly higher frequency than the frequency of the local field potential (Jeewajee et al., 2008), and this rhythmicity frequency increases with running speed (Hinman et al., 2016; Jeewajee et al., 2008; Stensola et al., 2012).

In addition to their robust firing relative to theta rhythm oscillations, grid cells show a loss of spatial selectivity during inactivation of the medial septum (Brandon et al., 2011; Koenig et al., 2011) which also causes loss of theta rhythmicity in the entorhinal cortex (Jeffery et al., 1995; Mitchell et al., 1982). This suggests an important role of theta phase coding in generating the allocentric location signal of grid cells. Recent studies have analyzed which specific population of medial septal neurons might regulate grid cell firing. The medial septum consists of three main cell populations, GABAergic, glutamatergic and cholinergic (Alonso & Kohler, 1984; Colom et al., 2005; Köhler et al., 1984; Shute & Lewis, 1967; Sotty et al., 2003). Of the three, GABAergic cells have been identified as the primary pacemaker of theta oscillations across both the hippocampus and entorhinal cortex (Brazhnik & Fox, 1999; Manseau et al., 2008; Serafin et al., 1996). Optogenetic activation of the septal GABAergic neurons drive local field potential oscillations in the medial entorhinal cortex but there is no change to grid cell spatial firing (Lepperod et al., 2021). In contrast, optogenetic inactivation of septal GABAergic neurons results in a large reduction in theta oscillatory power as well as a significant disruption to grid cell spatial periodicity (Robinson et al., 2021). In contrast, cholinergic and glutamatergic neurons have more moderate effects on ongoing theta rhythm oscillation and grid cell spatial firing. Chemogenetic activation of septal cholinergic neurons results in a small reduction in peak frequency in the medial entorhinal cortex and no change to grid cell spatial coding (Carpenter et al., 2017). While rhythmic optogenetic activation of septal glutamatergic neurons drives ongoing theta oscillation in the hippocampus (Fuhrmann et al., 2015; Robinson et al., 2016), optogenetic inactivation of this glutamatergic population of septal neurons results in no significant change to either theta oscillation frequency nor power but does show distortions of the grid spatial field (Robinson et al., 2021).

The mechanism of grid cell firing could depend upon different influences, including both transformation of sensory input that could drive egocentric boundary responses or path integration of self-motion. Behavioral data shows that sensory inputs versus self-motion integration can be combined when they give similar results or compete when they are inconsistent (Harootonian et al., 2022). The importance of sensory input in driving grid cells is supported by evidence that rotation of grid cell firing fields occurs with rotation of visual cues on the wall of a circular environment (Hafting et al., 2005; Savelli et al., 2017), and that grid cells show compression of the spacing between their firing fields in the dimension in which the walls of the environment are shifted closer to one another (Barry et al., 2007; Munn et al., 2020; Stensola et al., 2012). Research in mice shows a loss of spatial coding by grid cells when the animal is initially disorientated and visual cues are removed along with blocking of auditory and olfactory cues (Chen et al., 2016; Pérez-Escobar et al., 2016). In contrast, some grid cells have been shown to retain their spatially periodic firing pattern in darkness with only small changes in accuracy (Dannenberg et al., 2020; Hafting et al., 2005), suggesting the importance of non-visual cues or an additional role of path integration. However, grid cells show more accurate coding near environmental boundaries with reduced accuracy as a function of time or distance traveled from boundaries (Hardcastle et al., 2015), and they show reduced accuracy in darkness when other cues still remain (Dannenberg et al., 2020). Grid cells show a clear sensitivity to behavioral context and spatial geometry, losing their triangular/hexagonal firing pattern found in an open field environment when the rat is switched to running in a zig-zag pattern (Derdikman et al., 2009) or a spatial alternation task (Gupta et al., 2014). The importance of sensory input is further supported by data that grid cells lose spatial coding during inactivation of regions providing head direction input (Winter et al., 2015). These data indicate the ultimate influence of egocentric sensory input on grid cell firing. Thus, egocentric and allocentric representation of boundaries might interact with allocentric representation of location by grid cells and also by place cells as described in the following section.

1.5 | Allocentric coding of spatial location by place cells

Behavioral studies have explored tasks that require either egocentric or allocentric representations. For example, a classic study on the plus maze showed a dissociation between two different tasks that both involve starting from either the North or the South arm of the maze (Packard & McGaugh, 1996). In an egocentric task, the animal must always turn left whether starting from the North or the South, whereas in the allocentric task the animal must consistently go to the same location with respect to cues beyond the arena (i.e., the East arm; Guise & Shapiro, 2017). Lesions of the dorsal striatum impair the egocentric task (Packard & McGaugh, 1996), consistent with the presence of egocentric boundary cells in the dorsal striatum. In contrast, hippocampal lesions spare the egocentric task but impair the allocentric task, consistent with the allocentric coding of spatial location in the hippocampus. Similarly, finding the hidden platform in the Morris water maze is not impaired by hippocampal lesions when the animal always starts from the same location and can therefore use an egocentric strategy (Eichenbaum et al., 1990), but is impaired when the animal must navigate to that location from a range of different starting locations (Eichenbaum, 2017; Eichenbaum et al., 1990; Morris et al., 1982). Planning the correct spatiotemporal trajectory to the goal from multiple different start locations requires an allocentric representation of the animal relative to the task, as shown in different models (Erdem & Hasselmo, 2012, 2014; Ferbinteanu & Shapiro, 2003; Redish & Touretzky, 1998). In these models, a population of place cells provides an allocentric representation of a specific set of locations in a specific environment, allowing performance of the tasks.

The scope of this article cannot cover the full range of data on place cell firing properties but a brief summary will provide the context for subsequent discussions of computational modeling. After initial studies indicated that place cells fire based on spatial location (O'Keefe, 1976; O'Keefe & Dostrovsky, 1971), further studies showed firing responses within firing fields with diameters on the order of 20 cm during foraging in an open field environments (Huxter et al., 2008; Lever et al., 2002; Muller et al., 1987; O'Keefe & Burgess, 1996), and in local areas of linear tracks (O'Keefe & Recce, 1993), the 8-arm radial maze (McNaughton et al., 1983), or a spatial alternation task (Ainge et al., 2007; Kinsky et al., 2020; Wood et al., 2000). The firing of place cells can vary dependent on many factors including direction through the place field (Fenton & Muller, 1998) and the size of firing fields can differ and cells can have more than one firing field (Fenton et al., 2008). The position of an animal can be effectively decoded from the firing activity of hippocampal place cells (Brown et al., 1998).

Similar to the phase coding demonstrated by grid cells in deeper layers of entorhinal cortex, hippocampal place cells show robust phase coding of spatial location, in the form theta phase precession (O'Keefe & Recce, 1993). This phenomenon provides strong evidence for temporal phase coding in mammals. As the animal enters the firing field of a place cell, the spiking first occurs at late phases relative to theta rhythm recorded in the local field potential (Maurer et al., 2006; O'Keefe & Recce, 1993; Schmidt et al., 2009; Skaggs et al., 1996; Zugaro et al., 2005). As the animal runs through the firing field and exits, the phase of spiking shifts to earlier and earlier phases of theta. Across multiple neurons, theta phase precession often appears along with sequential spiking of neurons termed theta sequences

(Foster & Wilson, 2007), but phase precession can appear on the first trial in a novel environment, whereas theta sequences only appear later (Feng et al., 2015). Thus, models of place cells should consider phase coding as an important alternate hypothetical coding mechanism relative to rate coding.

Similar to grid cells, models of place cells have tended to focus either on sensory cues or path integration, but a few have combined these influences. A number of experimental studies show the importance of distal sensory cues for influencing place cells. Rotation of a differently colored cue card on the wall of a circular chamber causes rotation of place cell firing fields (Muller & Kubie, 1987), and starting an animal in darkness results in firing fields that differ from those seen when it enters in light (Quirk et al., 1990). This remapping of neuronal activity also occurs when the shape of an environment is changed in one room (Lever et al., 2002), or the same environment is placed into a different recording room (Fyhn et al., 2007), indicating the importance of distal cues. Hippocampal neurons including place cells can also show changes in mapping due to changes in sensory cues such as odors, reward, or tactile surface boundaries (Anderson & Jeffery, 2003; Wiener et al., 1989).

The support for influences of sensory input on place cell firing can be contrasted with evidence for the role of path integration, in which the self-motion signal including direction and speed is integrated to generate current location (McNaughton et al., 1996, 2006). The capacity for path integration is supported by data in rats showing that place cells can maintain their firing fields in the dark when a rat starts out in light conditions in the maze (Quirk et al., 1990) similar to grid cells in rats (Hafting et al., 2005). The importance of self-motion is also supported by comparisons of smaller place cell firing fields during active running compared to large, more diffuse place cell firing fields during passive movement on a train (Terrazas et al., 2005). The two mechanisms have been contrasted in an experiment using running from a start box to a goal location on a one-dimensional track that was shifted regularly (Gothard, Skaggs, & McNaughton, 1996; Gothard, Skaggs, Moore, & McNaughton, 1996). Some cells fired based on distance from the start location (supporting path integration), whereas others responded based on the visible box location (supporting influence of sensory input). Different models of place cell firing will be discussed further below in the section on modeling.

1.6 | Egocentric and allocentric representations in primate cortex

The research on egocentric spatial views in rodents relates to a long history of research in primates. Neurological investigations of effects of parietal cortex lesions in humans have demonstrated selective impairment of the perception of segments of spatial views, as in the case of parietal neglect that usually affects the left visual field after a right sided lesion affecting parietal cortex (Sidman et al., 1968). Consistent with this, early recordings from parietal cortex in non-human primates demonstrated neurons that code specific ranges of the direction of reaching movements generated by an animal (Georgopoulos, 1987; Kalaska et al., 1983; Mountcastle et al., 1975), or the perception of movements toward an animal (Caggiano et al., 2009; Rizzolatti & Fabbri-Destro, 2008).

Unit recordings in monkey hippocampus and parahippocampal regions have demonstrated neural responses to spatial views of the environment, known as spatial view cells (Georges-Francois et al., 1999; Mao et al., 2021; Robertson et al., 1998; Rolls et al., 1997, 1998). These neuronal responses are allocentric representations based on when the animal's gaze is focused on a specific segment of the external environment, as the neuronal responses do not change dependent on the orientation of the location relative to the animal's current position (Georges-Francois et al., 1999; Robertson et al., 1998; Rolls et al., 1997, 1998). Thus, a spatial view cell will respond when an animal looks at a particular location in a room, regardless of the animal's current location, head direction, or eye direction. Many neurons in monkey hippocampus, subiculum and entorhinal cortex also respond to facing location—firing when the animal's head direction is directed at a particular allocentric location independent of gaze direction (Mao et al., 2021). Both spatial view and facing location neurons differ from egocentric boundary cells, which depend strongly on the animals current location and head direction relative to the barrier (Alexander et al., 2020). Egocentric boundary responses also exist in monkeys, as some cells (Rolls & O'Mara, 1995) respond when the animal was facing the wall (restricted-view cells) or facing the center of the chamber (wide view cells), and a set of neurons with distinct egocentric boundary responses were shown in the same comprehensive study that showed both spatial view and facing location responses (Mao et al., 2021).

Electrophysiological recordings in non-human primates have also suggested a response analogous to grid cells, but rather than based on the animals allocentric position in the environment, these responses appear to depend on the current eye position of the animal (Bicanski & Burgess, 2019; Killian et al., 2012; Killian & Buffalo, 2018; Lewis et al., 2019; Meister & Buffalo, 2018; Rueckemann et al., 2021). In addition, neurons have been shown in non-human primates that respond to place, but these are much less frequent than spatial view responses (Ludvig et al., 2004; Mao et al., 2021; Wirth et al., 2017). This difference in number of place cells has been proposed to be due to the stronger reliance of primates on a narrow visual range of the fovea (Rolls, 2023). In contrast to more continuous theta during locomotion in rodents, non-human primates show brief bouts of theta rhythmicity during the onset of locomotion (Mao et al., 2021). Monkey single unit recordings in hippocampus, subiculum and entorhinal cortex show consistent phase locking to theta as well as gamma frequency in the local field potential (Mao et al., 2021), but only a few neurons show theta phase precession. Theta in the local field potential in monkeys also shows synchronization with the generation of saccadic eye movements (Hoffman et al., 2013; Jutras et al., 2013; Jutras & Buffalo, 2014; Katz et al., 2022), similar to phase reset with onset of stimuli in rodents (Givens, 1996; McCartney et al., 2004; Williams & Givens, 2003) and humans (Rizzuto et al., 2006).

Single units recorded in humans during virtual navigation show neuronal spiking responses similar to grid cells (Jacobs et al., 2013;

Nadasdy et al., 2017) and to place cells and spatial view cells (Ekstrom et al., 2003; Miller et al., 2013). Similar to monkeys, recordings in humans do not show the continuous theta rhythmicity during movement that is seen in rodents (Caplan et al., 2003; Ekstrom et al., 2005; Watrous et al., 2011, 2013), but instead show brief bouts of rhythmicity at lower frequencies that increases in power with movement speed (Bush et al., 2017; Ekstrom et al., 2005; Watrous et al., 2011). Theta rhythmicity in human hippocampus has also been shown to increase near the boundaries of the environment (Stangl et al., 2021). Recordings indicate that spiking responses in human hippocampus show theta phase precession relative to the theta rhythm in the local field potential (Qasim et al., 2021) and entorhinal neurons show phase locking to gamma (Nadasdy et al., 2022). fMRI activity in humans demonstrates a six-fold rotational symmetry in virtual worlds as predicted for grid cell responses (Doeller et al., 2010) which has also been observed in recordings of theta oscillations in the local field potential in the human entorhinal cortex (Maidenbaum et al., 2018). This sixfold symmetry is disrupted by virtual environmental barriers (He & Brown, 2019).

Neuronal activity in the human brain during virtual spatial navigation has been analyzed using functional magnetic resonance imaging. This reveals a robust neuronal activity in response to viewing complex spatial environments (Stern et al., 1996). Consistent with evidence for egocentric representations of boundaries in retrosplenial cortex of rodents, the retrosplenial cortex has been shown to be active for tasks that involve navigation based on spatial landmarks (Epstein et al., 2007; Epstein & Higgins, 2007; Sherrill et al., 2013). Different regions of the retrosplenial cortex show different functional associations, with episodic memory function in anterior regions and scene coding and navigation function in more posterior regions (Chrastil et al., 2018). The retrosplenial cortex has also been shown to be robustly activated when tracking distance back to the start location of a trajectory (Chrastil et al., 2015, 2016), consistent with a role in transforming an egocentric representation to an allocentric representation of distance. There is also a strong interaction of these structures with cortical structures representing optic flow (Sherrill et al., 2015). Thus, the neuronal activity in human cortex is consistent with the involvement of these structures in transformations from egocentric to allocentric representations.

2 | REVIEW OF MODELS OF SPATIAL COORDINATE REPRESENTATIONS

2.1 | Modeling of egocentric boundary cells

Egocentric boundary cells respond to a remarkable range of sensory input from the environment. As noted above, many egocentric boundary cells do not change their firing when the visual pattern on the walls is altered. In addition, the fact that these egocentric boundary cells can respond at distances up to 50 cm from the boundary wall suggest that they are guided by visual sensory input (Alexander et al., 2020). Computational models show that using synaptic modification with sparse coding constraints (Lian & Burkitt, 2021; Olshausen & Field, 1996, 2004) to form an efficient representation of visual input from the entire foraging trajectory within a population results in many simulated neurons that have responses similar to egocentric boundary cells that can respond similarly in circular and rectangular environments (Lian et al., 2022).

2.2 | Modeling of coordinate transforms in parietal cortex

Modeling the transformation from one coordinate frame to another, such as the egocentric to allocentric coordinate frame, can be performed by using what are referred to as gain field representations (Bicanski & Burgess, 2018; Pouget & Sejnowski, 1997; Salinas & Abbott, 2001). Gain field representations allow coordinate transformations by using a nonlinear (usually multiplicative) interaction between an input representation in one coordinate system (e.g., retinotopic) and another input representing a different coordinate system (i.e., eye position). If the inputs are basis functions (e.g., Gaussians for the retinotopic response, and sigmoids for the eye position), then the combination can act as a basis function for a wide range of different outputs (Pouget & Sejnowski, 1997). However, this requires that the full range of retinotopic inputs should be multiplied by the full range of eye positions. This then allows an output to be learned that involves a linear combination of the two inputs such as generating a reaching response with an angle $x + y$ that adds the angle of the visual cue (x) and the angle of the eye position (y) to generate the necessary angle of reaching ($x + y$) as described in work by Salinas and Abbott (2001). These authors point out that the multiplicative interactions used in gain fields could arise from multiplicative interactions due to nonlinear interactions of NMDA conductances on adjacent synapses on the dendritic tree (Mel, 1993), or from multiplicative interactions due to center-surround interactions of recurrent synapses (Salinas & Abbott, 1996, 1997, 2001).

2.3 | Neural activity relevant to gain field transformations

The hypothesis of gain field transformations predicts conjunctive spatial representations that should show a change in firing rate that combines sensitivity to one spatial variable (e.g., egocentric position of a wall or cue) with an increase or decrease in firing rate (i.e., a gain modulation) based on a second variable such the gaze direction of the animal (Andersen et al., 1985). These types of conjunctive responses have been observed in a number of regions. Neurons in parietal cortex of rodents code the egocentric angle to behaviorally relevant visual landmarks and the animal's allocentric heading orientation simultaneously (Wilber et al., 2014). Retrosplenial neurons also exhibit changes in response to repeated visual landmarks that appear at different spatial positions (Fischer et al., 2020; Mao et al., 2020; Powell et al., 2020) as a conjunctive code of a visual cue and its relative location. A change in firing rate was observed for the response to repeated local features during running along a familiar route (Alexander & Nitz, 2015, 2017; Nitz, 2012). Modulation by position along a route has been shown to alter firing rate for both egocentric turns and higher-order cognitive variables such as choice availability in secondary motor cortex (Olson et al., 2020).

Similar to these examples, egocentric boundary cells in lateral entorhinal cortex, postrhinal cortex, and retrosplenial cortex exhibit co-modulation by allocentric head direction (Alexander et al., 2020; Gofman et al., 2019; Jacob et al., 2017; LaChance et al., 2019, 2022) supporting proposed mechanisms for translation between coordinate systems in network models (Bicanski & Burgess, 2018; Byrne et al., 2007). As noted above, combinations of neurons with conjunctive gain-field modulation can approximate nonlinear coordinate frame transformations (Bicanski & Burgess, 2018; Pouget & Sejnowski, 1997; Pouget & Snyder, 2000). Thus, there is support for a role of gain field modulation in mediating coordinate transformations.

2.4 | Modeling of egocentric to allocentric transformation of boundary cells

The model of transformations from egocentric to allocentric maps by the Burgess group (Bicanski & Burgess, 2018; Byrne et al., 2007) used an egocentric representation of barriers that was multiplied by a range of representations of head direction, based on neural evidence for conjunctive codes supporting gain field modulation. In this framework, the input of any specific current head direction could multiply the egocentric barrier input to allow a transformation to the same stable allocentric representation of the barriers. This framework requires representations of both barriers and head direction that uses large vectors of smooth firing rate that are combined in an extensive weight matrix for the transformation to allocentric coordinates. This representation also requires experiencing boundary segments at all distances and directions at least once in the environment to create the necessary maps for all distances and directions, as the model does not automatically interpolate or extrapolate to previously unlearned distances and directions. This developmental learning phase has not been modeled yet. An alternate framework for egocentric to allocentric transformations is summarized below in section 3.

2.5 | Prior modeling of the allocentric firing of grid cells

Despite the strong evidence for the importance of sensory input in driving grid cells, many existing models of grid cells instead focus on the phenomenon of path integration, in which the grid cell firing field is updated based on the animal's current movement velocity, consistent with coding of running speed in hippocampus (McNaughton et al., 1983), entorhinal cortex (Dannenberg et al., 2019; Kropff et al., 2015; Wills et al., 2012) and retrosplenial cortex (Carstensen et al., 2021). Path integration was the primary mechanism used for generating grid cell firing fields in all of the attractor dynamic models of grid cells (Burak & Fiete, 2009; Fuhs & Touretzky, 2006; Guanella et al., 2007; McNaughton et al., 2006), as well as the oscillatory interference models of grid cells (Burgess, 2008; Burgess et al., 2007; Hasselmo, 2008; Zilli et al., 2009; Zilli & Hasselmo, 2010). Integration of velocity in these models allows updating of the grid cell firing field relative to the starting position of that session. This mechanism suffers from potential accumulation of error, but this can be reduced by resetting the network based on sensory input from place cells as was performed in a hybrid model combining oscillatory interference and attractor dynamics (Bush & Burgess, 2014). Other models have focused on the ongoing update of grid cells by sensory input from place cells (Kropff & Treves, 2008; Si et al., 2012), consistent with evidence that inactivation of place cells reduces the spatial specificity of grid cells (Bonnevie et al., 2013), whereas loss of grid cell specificity during medial septum inactivation (Brandon et al., 2011; Koenig et al., 2011) does not abolish place cells (Brandon et al., 2014).

2.6 | Prior modeling of the allocentric firing of place cells

The review of behavioral data above indicates the behavioral importance of an allocentric representation of spatial location by place cells. But how can this allocentric representation be formed? There are a number of models of the formation of allocentric spatial representations. Early models proposed that place cells could be formed based on configurations of sensory cues (Brown & Sharp, 1995; Shapiro & Hetherington, 1993). Another model proposed that intrinsic network dynamics generate an internal place cell map, which is then anchored to specific external sensory features (Samsonovich & McNaughton, 1997). Another set of models proposed that place cell representations are associated with different combinations of allocentric boundary cells via a gain field transformation of rate coding vectors provided by egocentric boundary cells (Bicanski & Burgess, 2018; Byrne et al., 2007; Hartley et al., 2000). Alternatively, the place cell representation could be formed by summation of the input from grid cells, regardless of the mechanism for grid cell formation (Fuhs & Touretzky, 2006; Hasselmo, 2009; O'Keefe & Burgess, 2005; Rolls et al., 2006; Solstad et al., 2006). A further possibility described in more detail below is that place cells arise from a transformation of phase coded representations from the entorhinal cortex. In this framework, the place cell representation could be formed and reactivated by a phase coded representation as summarized in the following section. In the latter framework, the entorhinal grid cells could provide systematic phase shifts that could explore the full possible range of spatial translations and rotations.

3 | A PHASE MODEL USING BOUNDARY CELLS TO DRIVE GRID CELLS AND PLACE CELLS

This section describes a model of the transformation from egocentric to allocentric coordinates that uses a temporal phase code rather than a rate code. The existence of temporal phase coding is strongly supported by the phenomenon of theta phase precession by entorhinal grid cells (Climer et al., 2013; Hafting et al., 2008; Jeewajee et al., 2014) and hippocampal place cells (Huxter et al., 2008; Ning et al., 2022; O'Keefe & Recce, 1993; Skaggs et al., 1996). This framework proposes that features such as boundaries can also be represented by phase of firing relative to theta or gamma rhythm oscillations in the retrosplenial cortex or entorhinal cortex, rather than mean firing rate. This is compatible with evidence that retrosplenial egocentric boundary cells and other neurons show selective phasic firing relative to theta rhythm as well as gamma frequency coupling to hippocampal theta oscillations (Alexander et al., 2018, 2020), though boundary responses can appear in the absence of theta (Koenig et al., 2011). In this framework, the coding of a particular previous location in a particular environment could then be stored by a neuron such as a place cell that has dendritic dynamics that are sensitive to the specific phases of a set of boundary cells. The computation of other allocentric positions relative to this coded position could then be performed by an array of entorhinal grid cells that perform phase shifts corresponding to translation relative to this initial location. The model uses oscillatory dendritic dynamics similar to the oscillatory interference model of grid cells (Burgess, 2008; Burgess et al., 2007). However, the current model does not involve integration of movement velocity by oscillatory dynamics. Instead, this framework involves a coding a phase shift dependent on the egocentric distance to environmental barriers (Raudies & Hasselmo, 2015) as coded by egocentric boundary cells. Note that this mechanism resembles the phase resetting of oscillations induced by visual input in models that used a combination of velocity updating and visual sensory input (Bush & Burgess, 2014). However, here the input phase is representing sensory input proposed to occur continuously at all time points. Instead of summing oscillations that have integrated position by changes in frequency, the model sums oscillations with phases that represent location dependent sensory input with oscillations representing a previously stored set of input phases. This interaction of oscillations is proposed to be mediated by a stored dendritic sensitivity to phase dynamics generated by input rather than an interaction of ongoing oscillations. This idea is described in further detail below and in the following figures.

3.1 | Mathematical example

Figure 4 illustrates the basic idea of the mathematical computation of current allocentric location from egocentric coordinates. Figure 4a shows coding in egocentric coordinates of the position of the barrier relative to the front, back, left and right of the animal at a particular time point when an animal first enters the environment (for simplicity, this is considered to be the lower left corner of environment with direction north). In this example, the animal sees the egocentric position of the center of each environmental barrier (indicated by gray

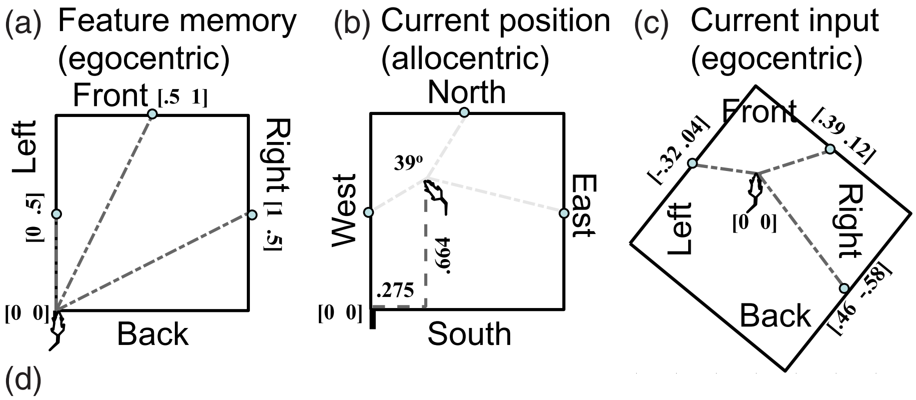

$$\begin{bmatrix} 0 & 0.5 & 1 \\ 0.5 & 1 & 0.5 \\ 1 & 1 & 1 \end{bmatrix} = \begin{bmatrix} cos(39^\circ) & -sin(39^\circ) & 0.275 \\ sin(39^\circ) & cos(39^\circ) & 0.665 \\ 0 & 0 & 1 \end{bmatrix} \begin{bmatrix} -0.32 & 0.39 & 0.46 \\ 0.04 & 0.12 & -0.58 \\ 1 & 1 & 1 \end{bmatrix}$$

A=B*C

FIGURE 4 Mathematical computation of current allocentric location from egocentric coordinates. (a) The animal is assumed to have a memory of barrier feature locations (circles on walls) in egocentric coordinates shown here as memory vectors (gray dash-dot lines) relative to its previous position during an initial encounter with the environment. (b) The information on egocentric feature coordinates in memory (a) and at the current time (c) can be related by an affine transformation matrix B that codes current allocentric position (dark gray dashed lines) of the animal relative to the position of the previous memory (one position relative to another position). (c) At any given time, the current egocentric barrier feature is coded in egocentric coordinates (gray dash-dot lines) relative to its current position. (d) Matrix multiplication generates the memory egocentric vectors in (the egocentric coordinates in array A). This is equal to the result of multiplying the affine transformation matrix B by the current egocentric vectors (the egocentric coordinates in array C). The affine transformation matrix includes the allocentric coordinates corresponding to the rotation of the agent relative to initial position (39°) and the allocentric translation *dx* and *dy* of the agent relative to the start location

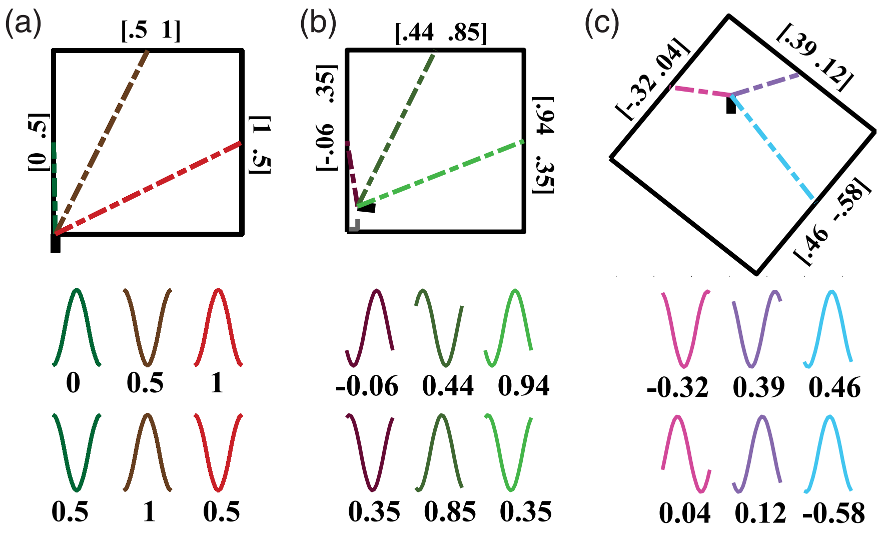

$$\begin{bmatrix} cos(39°) * (-0.32) + & -sin(39°) * (0.04) + & 0.275 * (1) \\ sin(39°) * (-0.32) + & cos(39°) * (0.04) + & 0.665 * (1) \\ 0 * (-0.32) + & 0 * (0.04) + & 1 * (1) \end{bmatrix} = \begin{matrix} 0.0 \\ 0.5 \\ 1 \end{matrix}$$

FIGURE 5 Example of the representation of the numbers in Figure 4 by the phase of waves. (a) The colored *x*,*y* dimensions of vectors at top match the phases of waves representing x and y below. (b) A small shift in position results in a small shift in phase of the waves. (c) A larger shift in position and rotation results in very different egocentric coordinates. The colors of these egocentric vectors match the waves representing these vectors below. (d) Summary of the matrix computations that relate one column of input to one column of output. These could result from dendritic dynamics allowing multiplicative influences on phase in local areas of the dendrite

dash-dot lines), and this is presumed to activate responses of egocentric boundary cells that fire at a specific phase relative to network theta. The numbers in the figure show the egocentric Cartesian coordinates (*x*,*y*) of each of three features at the center of each of three walls, which are coded in the array in Figure 4d as [0; 0.5], [0.5; 1], [1; 0.5]. In this example, this first view of the environment is considered to be stored as a memory of the environment, potentially by intrinsic dynamics of a neuron biasing toward responding to a specific phase.

Figure 4b shows a later time point when the animal is at a different allocentric position that is translated by $x = 0.275$ and $y = 0.664$ (gray dashed lines) and rotated by 39 degrees. How can the animal determine this new position relative to the starting point? Figure 4c shows the egocentric coordinates of the wall features relative to the animal at this new point (dark gray dash-dot lines). These are coded in Figure 4d as [−0.32; 0.4], [0.39; 0.12], [0.46; −0.58]. The computation in Figure 4d shows the mathematical relationship between the memory of the first egocentric feature coordinates A (Figure 4a), and the current egocentric feature coordinates C (Figure 4c). Note that these egocentric coordinates are related by the affine transform matrix B, which codes the current allocentric position of the animal show in Figure 4b. This affine transformation matrix includes four values in the upper left (rows 1–2 and columns 1–2) that code the rotation of the animal's allocentric head direction (39 degrees) as well as two values in the upper right (rows 1–2, column 3) that code the allocentric translation *dx* and *dy* of the animal relative to the memory of start location.

In this framework, computing the current allocentric position and angle involves computing the affine transform matrix B. This matrix B could be obtained mathematically from the feature coordinates from Figure 4a,c, to generate the current allocentric position of the animal relative to the animal's previous position in the environment. This mathematical computation of current allocentric position could be performed by multiplying the pseudoinverse of the array of egocentric coordinates by the egocentric memory coordinates to obtain an affine transformation matrix $B = C \times A^{-1}$. However, it is not clear that neural circuits could compute the pseudoinverse.

Alternately, the network could test in parallel numerous affine transform matrices to find the one that best fits the original memory. That is what we propose here, though the exact physiological mechanisms are not fully clear. The basic idea is that each entorhinal cell receives current egocentric information (Figure 4c) and an egocentric memory of environment (Figure 4a), and each entorhinal cell has distinct individual dendritic phase shifting properties that represent a range around one possible affine transformation. The dendritic physiological mechanisms that could implement this mathematical transformation are not completely clear. However, this could involve representation of values by the phase of theta waves of membrane potential on the dendrite induced by synaptic input from areas such as retrosplenial cortex. These inputs could be influenced by dendritic mechanisms that cause phase shifts corresponding to the affine transformation matrix. These phase shifted inputs then interact with theta waves induced by separate dendritic properties or synaptic input that represent the original memory of the environment from the hippocampus. In the model, the theta waves induced by synaptic input are represented by cosine functions that are summed, and evaluated for crossing a threshold. This causes spatially phasic interactions similar to the oscillatory interference model of grid cell (Burgess, 2008; Burgess et al., 2007). The entorhinal cells with phase shifts that cause the phase induced by retrosplenial input to best match the phases induced by memory from hippocampus are the ones that are activated at a current moment, firing as grid cells. In this manner, the entorhinal cells with phase shifts corresponding to the appropriate affine transformation are activated and thereby code the appropriate affine transformation for current position. Entorhinal cells with different phase shifts will show different spatial phases.

Figure 5 shows how the numerical values of the vectors shown in Figure 4 can be represented by theta waves modeled as cosine functions with specific phases that are proposed to be induced by input to entorhinal cortex from retrosplenial or postrhinal cortex and from hippocampus. Figure 5a shows the phase of theta waves (cosine functions) representing the memory from hippocampus for the egocentric vectors between the starting location 0,0 in the lower left and the three different features on the walls. Each vector is coded with a color that matches the color of the theta waves (cosines) that represent the vector by their phases (i.e., the first two waves shown in dark green correspond to the vector $x = 0$, $y = 0.5$). The other vector colors match the phases of the other wave pairs. The waves could arise from synaptic influences on voltage-sensitive membrane conductances such as *h* current or *M* current that alter the phase of membrane resonance (such as cAMP activation of h current), or could be due to network activation of excitatory and inhibitory currents. Notably the experimental reduction of *h* current blocks the shift of grid cell spacing and change in slope of speed coding that normally occurs in response to movement of barriers (Munn et al., 2020). Here, the vectors are represented by two dimensions at 90 degree angles, but in Figures 6 and 7, they will be represented by three dimensions at 120 degree angles. Figure 5b shows that a small shift in location that causes a small shift in egocentric vectors corresponds to a small shift in phase of the waves. Figure 5c shows theta waves (cosine function) representing current egocentric vectors between location and features that could be induced by synaptic input from egocentric boundary cells in retrosplenial or postrhinal cortex. The current egocentric input in Figure 5c has a large difference in rotation and translation from Figure 5a, resulting in a larger difference in phase. The color of the vectors again matches the color of the waves with different phases. Figure 5d illustrates the components of the affine transformation that generate the first column of Figure 5a from the first column of Figure 5c. The exact mechanisms for such a phase shift are not clear, but could involve the dendritic currents causing a shift of the phase of dendritic theta waves that could be due to intrinsic properties of the *h* current and potassium

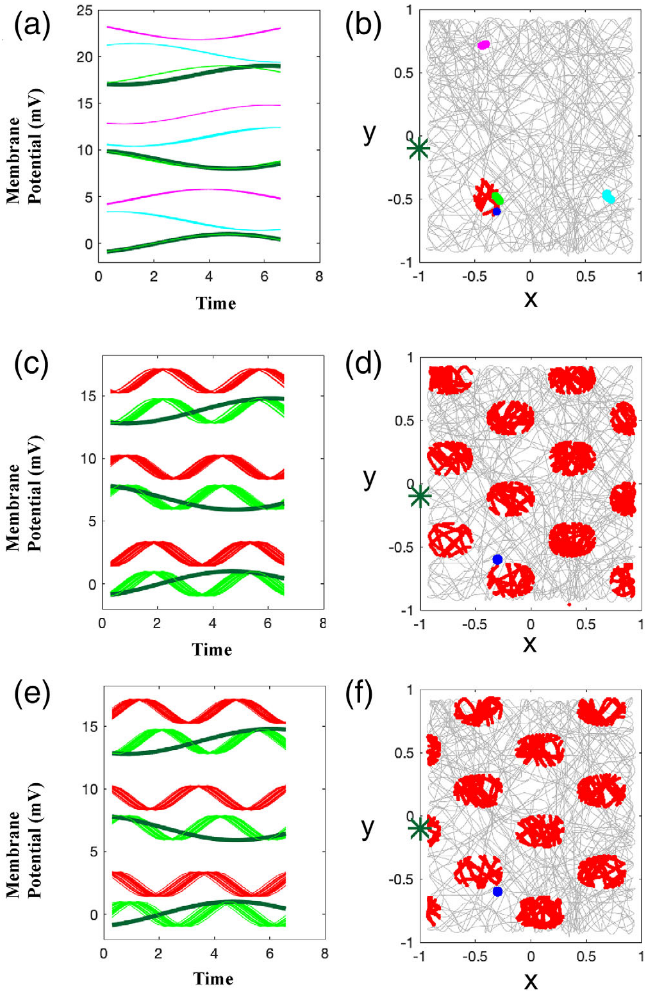

FIGURE 6 Simulation of place cells and grid cells with phase codes shown for one feature on the West wall for simplicity (dark green asterisk on West wall). (a) Memory of a location in lower left of environment is stored by phases of dendritic sensitivity representing distance to the feature (dark green theta waves—cosine functions). Examples of phases of theta waves for locations that match the memory are shown by light green curves, which match the dark green curves. Examples of phases for locations that do not match are shown in magenta and cerulean. (b) As the animal forages (gray lines in b), the locations generate different phases for egocentric coordinates in (a). The memory location is shown as a blue dot. The locations corresponding to the light green wave phases in (a) are shown as dots in light green. The broader range of locations with input matching the dark green curves are marked by red dots. The cerulean or magenta dots show other locations not in place field that correspond to the cerulean and magenta waves. (c) For a grid cell simulation, the synaptic input of egocentric feature distance activates dendritic dynamics with high frequency oscillations (red and light green cosine functions with two cycles). The red and light green waves shown here have peaks that come closest to matching the peak phase of the lower frequency memory waves (dark green), and therefore generate spikes shown in (d). (d) Grid cell firing locations corresponding to all matching phases are shown in red (where the red wave peaks driving the light green wave peaks best match the dark green wave peaks. (e) For a different grid cell, the red cosine functions again show the responses to egocentric synaptic input at example input location phases that successfully drive the grid cell. Because this grid cell has different dendritic dynamics that cause a translational phase shift, these red inputs are shifted in phase by the dendrites to create the light green waves (different phases of red and light green cosine functions). The figure shows the light green waves that have peaks that best match the peaks in the memory waves (dark green) and drive spikes (red dots in f). (f) The grid cell firing locations corresponding to all matching locations are shown in red. The dendritic phase shift between red and light green causes these locations to be out of phase relative to Figure 6d. Thus, a different set of red firing locations match the memory due to the dendritic phase shift.

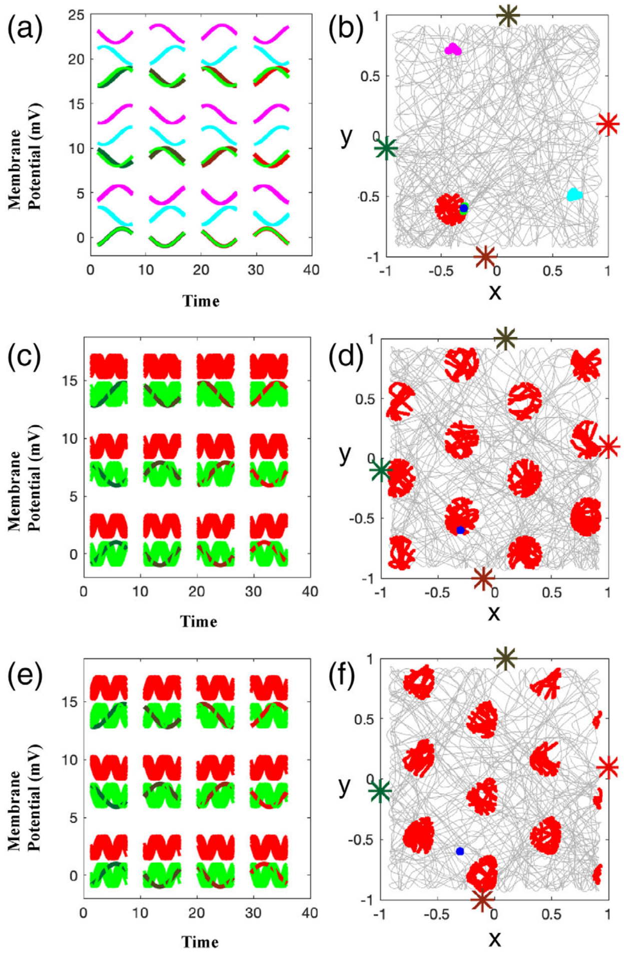

FIGURE 7 Simulation of place cells and grid cells based on phase coding of four wall features. (a) The memory of a location in the lower left of environment is stored as phases of dendritic sensitivity representing different distances to four walls. Thus, four columns with three cosine functions in each column represent distances from current location to each of four features labeled with dark green, olive, brown and red. As the rat forages, the current egocentric coordinates are represented by 12 input phases (light green). Phases for other locations that do not match are shown in magenta and cerulean. (b) The place cell plot shows red dots for all locations when input phases are close to memory phases. Light green dots show closest examples corresponding to the green curves in Figure 7a. (c) The place cell phase code sent to entorhinal cortex sets phase dynamics for an individual location with a specific distance to each feature represented by cosine function shown in dark green, olive, brown, and red. The input of current phase (red cosine functions) are phase shifted by entorhinal membrane dynamics to cause dendritic dynamics (light green waves) that match the dendritic sensitivity dynamics coding features (dark green, olive, brown, red). Because of this phase shift, the best match occurs for phases where the peak of the light green waves does not match the peak of the red waves. (d) When the light green dendritic dynamics match stored feature dynamics the grid cell fires a spike (all matching locations shown as red dots). (e) A different grid cell has dendritic dynamics that cause less phase shift than part d resulting in a similar phase between the red phases and the light green phases. (f) The red dots show all locations of best matching dynamics. Note the translational phase shift relative to the red dots in (d) due to the difference in dendritic phase shift between the red and light green lines in (c).

currents that influence the relative inductance and resistance of the dendrite.

3.2 | Generation of a place cell response

As described above and in Figures 4 and 5, the phase of firing of retrosplenial egocentric boundary cells could represent the current distance of the animal from features such as the middle of each wall. This could be matched to a previously learned set of phases that have been stored by the intrinsic sensitivity of dendritic dynamics in a place cell or by synaptic input from a specific hippocampal place cell. The matching of current sensory input along the trajectory to a particular stored pattern of oscillatory dynamics is shown in Figure 6a.

As the rat forages in the environment, the trajectory of the foraging rat is shown in light gray in Figure 6a. For each location along this trajectory, a set of input curves are generated representing input from phase coding of the egocentric position of the single feature on the barrier. Thus, each current location along the trajectory is represented by a phase code representing distances to one feature (dark green asterisk) on one wall. In Figure 6a, the memory of a location in the bottom left of the environment is stored by phases of theta waves (dark green cosine functions in Figure 6a) that represent different distances to the feature on one wall. Note that these phases represent the *x*,*y* vector projected onto three vectors at 120° angles, one in the direction of dimension *x*, and the other at 120° angles. The stored phase code of this single location relative to this single feature is shown in dark green curves in Figure 6a and a dark blue dot in lower left of Figure 6b. The exact mechanism of storage is not clear, but could involve long-term phosphorylation of h current channels that can be reactivated by synaptic input.

This simulation can generate a place field type response. At all locations on the gray trajectory, the cosine functions (theta waves) induced by synaptic input representing current egocentric input are summed with the cosine functions representing specific phase properties associated with the stored location, and the summed cosines are evaluated for crossing a threshold. This sum crosses the threshold when the rat is in locations shown by light green dots in Figure 6b, where synaptic input from egocentric boundary cells generates dendritic dynamics (theta waves) shown as light green curves in Figure 6a. In these locations, the simulated neuron generates a spike because the current input phases (light green) are close to the memory phases (dark green) in Figure 6a, driving the light green dots in Figure 6b. For clarity, the light green curves in Figure 6a show a small subset of a larger number of matches.

Beyond the few examples shown in light green, there are many additional cases in which summation of input cosine functions close to the stored dark green cosine functions crosses a threshold to cause spiking activity. The broader range of matching occurs when the agent is in locations (in Figure 6b) shown as red dots, resulting in spiking in a localized area similar to a place cell firing field. The size of the firing field depends on the threshold used to evaluate the sum or multiplication of the input curves and the curves coded by dendritic dynamics.

Note that data on egocentric boundary responses suggests broader tuning at greater distances (Alexander et al., 2020), which could be reflected in greater variance in firing at greater distances from the walls (Hardcastle et al., 2015).

Figure 6a separately shows the stored phase code curves (cosine functions) in magenta and cerulean for two other place cells that differ in location and distance from the dark green feature relative to the dark green phase codes. These cells could fire at different times when the animal is close to these stored phases. Figure 6b uses the same colors to show the location where these different phase code curves were generated. It can be seen in Figure 6a that these phase codes are not similar to the memory represented by specific waveforms shown in dark green.

Note that the simulation is not showing all possible rotations, but focuses on representing translations for one orientation of the rat. The difference in head direction on different trajectory could be decoded by head direction cells modulating the affine transformation matrix as shown in Figures 4d and 5d. This review paper does not have space to go into all the details and potential extensions of this newly developed model.

3.3 | Mechanism of dendritic dynamics

The dendritic dynamics shown in dark green in Figure 6a could be implemented by altering second messenger pathways that alter the time constant of various dendritic membrane channels to influence dendritic dynamics such as the hyperpolarization activated cation current (*h* current) or voltage-sensitive potassium currents such as the *M* current (Hasselmo et al., 2021). These dendritic membrane potential dynamics could include oscillatory dynamics such as those observed in hippocampus and entorhinal cortex with intracellular recording from cell bodies in slice preparations (Dickson et al., 2000; Fransen et al., 2004; Haas et al., 2007; Haas & White, 2002; Giocomo et al., 2007) and in vivo intracellular recordings from behaving animals (Domnisoru et al., 2013; Harvey et al., 2009; Leung & Yim, 1986; Schmidt-Hieber & Hausser, 2013). The membrane potential dynamics of entorhinal stellate cells have been shown to vary systematically along the dorsal to ventral axis of entorhinal cortex, including differences in frequency of resonance and subthreshold oscillations (Giocomo et al., 2007; Giocomo & Hasselmo, 2008, 2009) as well as the sensitivity to oscillatory input (Shay et al., 2016) and the time constant of rebound spiking (Ferrante et al., 2017). Knockout of the HCN1 subunit of the h current has been shown to alter the size and spacing of grid cell firing fields (Giocomo et al., 2011), and knockout of TRIP8b that blocks *h* current blocks the change in grid cell spacing and change in slope of speed cell coding that normally occurs with movement of barriers (Munn et al., 2020).

The dendritic dynamics mediated by membrane conductances such as *h* current could be altered for specific phase sensitivity by metabotropic glutamate receptors that can alter cAMP levels and modulate the time constants of the hyperpolarization activated cation current (*h* current) (Wainger et al., 2001; Wang et al., 2002) or the calcium-dependent potassium current (AHP current; Lancaster et al., 2006) to alter the phase and frequency of dendritic oscillations or other waveform shapes. In previous work, dendritic dynamics of oscillations or rebound spiking were proposed to underlie grid cell firing generated by path integration (Hasselmo & Shay, 2014). The framework presented here uses similar membrane potential dynamics but focuses on the translation of a phase code induced by synaptic input representing sensory features, rather than updating of current position based on path integration. A particular pattern of dendritic dynamics could potentially be stored in a more stable manner in the form of the expression or phosphorylation of a particular pattern of membrane channels in the dendrites of a neuron that gives the neuron lasting sensitivity to that dynamical pattern. Alternatively, synaptic input from other neurons could induce dendritic dynamics that activate mGluR receptors to change membrane potential dynamics via h current (Wainger et al., 2001; Wang et al., 2002). Or local circuits of excitatory and inhibitory neurons could induce phase dynamics that interact via multiplicative interactions of NMDA conductances (Poirazi et al., 2003).

3.4 | Generation of entorhinal grid cells

As described above, the intrinsic properties of grid cells are proposed to implement phase shifts that correspond to specific affine transformation matrices. The example in Figure 4d shows the affine matrix, which could determine allocentric location and angle. This matrix corresponds to a specific set of phase shifts. As noted in the discussion of Figure 4d, it may be biologically unrealistic to compute this matrix using a pseudo-inverse. As an alternative, the determination of current allocentric location could involve sampling an array of many possible translations, in which the retrosplenial boundary cell input to the hippocampus is simultaneously shifted to different amounts across a range of phase delays by a population of entorhinal grid cells that each individually represent one of a range of different phase shifts (as well as rotations). In this framework, a coordinate transformation would be mediated by a matrix multiplication process (as in Figure 5d) that involves shifting of phase rather than alteration of firing rate. A phasic representation of current sensory input in boundary cells could be matched to a stored memory in place cells by a large network of grid cells that each represent a matrix representing one of many possible translations (and rotations) of the egocentric sensory input for comparison with the dendritic dynamics representing a previously stored memory of the phases associated with a specific location.

The role of grid cells in testing translation for different locations is summarized in Figures 6 and 7. Figure 6c shows how a grid cell could mediate an interaction of egocentric boundary distances related to positions stored by the place cell. For example, the place cell phase code could be sent to entorhinal cortex to set phase sensitivity for all grid cells (dark green lines in Figure 6c). The simulated rat forages along the curvy gray trajectory shown in Figure 6d and generates different input phase dynamics at each location. The effect of egocentric synaptic input on dendritic dynamics are shown for a subset of locations as red theta waves (cosine functions) in Figure 6c. The difference from Figure 6a is that the synaptic input causes dendritic dynamics that have higher oscillatory frequencies, consistent with effects of *h* current that cause membrane potential oscillations of different frequencies (Garden et al., 2008; Giocomo et al., 2007; Haas & White, 2002). The example also differs from Figure 6a in that Figure 6a shows an array of three place cells each with different stored phases representing stored input at different locations, whereas Figure 6c–f show two grid cells with internal phase shifting dynamics that cause them to fire at different locations relative to the same stored position (same dark green curve).

Figure 6c shows the synaptic input inducing red cosine functions causes internal dendritic dynamics shown in light green that have the same phase as the red cosines. When the phase peaks of light green dendritic dynamics best match the peaks of the lower frequency dendritic dynamics associated with the memorized location (dark green cosines), then the sum of these waves in the neuron crosses a membrane potential threshold and generates a spike. The location of the animal for a wide range of locations where the input dynamics match the memory dynamics are shown as red dots in Figure 6d. This shows that the simulation can replicate properties of entorhinal grid cells. Because the input dynamics (red cosines) are higher frequency, their multiple peaks match the slower memory dynamics at a multiple different locations. The full range of matching points are shown by red dots in Figure 6d. The red dots have a spread of spatial phases consistent with the spread of temporal phases in Figure 6c.

In Figure 6c, the red cosines induced by synaptic input and light green curves resulting from intrinsic dendritic dynamics match in phase. However, the simulation in Figure 6e illustrates the effect of different intrinsic dendritic dynamics that shift the dendritic response to input (red cosines) and generate dendritic responses with different translational phase shifts (light green cosines). This is based on the fact that experimental data shows that neurons in medial entorhinal cortex have different membrane potential dynamics mediated by *h* current and potassium conductances that can alter the frequency and phase of neuronal oscillations (Boehlen et al., 2010; Dodson et al., 2011; Garden et al., 2008; Giocomo et al., 2007; Giocomo & Hasselmo, 2008, 2009; Heys et al., 2010; Pastoll et al., 2012; Shay et al., 2012), building on the initial work on these properties in entorhinal cortex (Erchova et al., 2004; Haas & White, 2002).

The effect of the dendritic phase shift proposed to be caused by intrinsic properties is shown in Figure 6e. In this case, the dynamics (red cosines) induced by egocentric boundary cell input are shifted by intrinsic dendritic conductances to cause a phase shift in dendritic dynamics (light green cosines in Figure 6e). Figure 6e shows that the dendritic dynamics shown as light green cosines that best match the dynamics induced by the memory location (dark green cosines) are similar to the light green cosines in the previous figure Figure 6c. However, Figure 6e also shows that the phases induced by input phases (red cosines) that induce these light green cosines are very different (compare red cosines in Figure 6e with those in Figure 6c). This is proposed to be due to different grid cells having different dendritic conductances that generate dynamics that cause differences in phase shift. This will result in a different phase relationship between the response (red cosines) to boundary cell input and the intrinsic dendritic dynamics (light green traces) for a specific location, and therefore results in a shift in the firing location of the grid cell (Figure 6f). As shown in Figure 6f, the locations that best drive the grid cell (red dots in Figure 6f) correspond to very different locations than the ones that drive the grid cell in Figure 6d (note difference in spatial phase of the red firing fields).

Figure 7 illustrates a similar example, but for a larger number of features on walls in this case four features shown as asterisks on each wall of the environment. Figure 7a shows the same properties for a place cell, but in this case instead of three dark green curves representing the dendritic sensitivity for a location, there are 12 curves corresponding to three phase codes (rows) in four columns that represent four different features (coded as dark green, olive, brown and red). These four features are shown as asterisks of different colors on different walls. The inputs are generated for each point on the gray trajectory in Figure 7b in the form of 12 phases corresponding to the egocentric boundary coding of the distance to each of the four wall features. Figure 7c,d show the generation of a grid cell based on the phase coding of the four walls. In Figure 7c, the high frequency red theta waves induced by egocentric synaptic input undergo a systematic phase shift due to dendritic dynamics, resulting in the high frequency light green theta wave cosines that are shifted from the red waves. The summation of these light green cosines with the egocentric cosine functions (dark green, olive, brown, red) crosses threshold when the cosines are in phase with each other, corresponding to the red dots in Figure 7d. Figure 7e,f shows a different grid cell in which the red cosines match the light green cosines such that the cell fires in a different set of locations than in Figure 7d, corresponding to the input phases shown as red cosines in Figure 7e and corresponding to the locations shown as red dots in Figure 7f. The plots with a larger number of walls generate more circular grid cell firing fields than the single wall example shown in Figure 6.

This description provides a preliminary framework for showing how a temporal phase code rather than a rate code could be used to transform the egocentric representation of position relative boundaries (Alexander et al., 2020) into allocentric representations by grid cells and place cells. As noted above, the matching of the oscillatory dendritic dynamics by summation and thresholding is very similar to the oscillatory interference model of grid cells (Burgess, 2008; Burgess et al., 2007), but uses a phase code dependent on the egocentric distance to environmental barriers (Raudies & Hasselmo, 2015) proposed for egocentric boundary cells. This resembles previous phase resetting of oscillations by visual input (Bush & Burgess, 2014), but the interaction of oscillations is proposed to be regulated by intrinsic dendritic dynamics. Thus, rather than correcting a continuous position determined by path integration, the position representation is generated by a phase code from sensory input that interacts with stored dendritic sensitivity dynamics with differential phase shifts mediated by cellular properties within different neurons in the medial entorhinal cortex.

4 | CONCLUSIONS

This paper reviews data on egocentric boundary cell representations in rodents and the relationship to allocentric representations of boundaries by boundary vector cells, and the coding of location by grid cells and place cells. The review also addresses the physiological data on coding different coordinate frames in humans and non-human primates. Existing models have addressed these coordinate transformations using gain field representations that match sensory responses. However, these gain field representations would require extensive learning of numerous distances and directions relative to arena walls. As an alternative, a phase code model is sketched out that could allow phase coding of egocentric distance to barriers to generate allocentric representations by place cells and grid cells. In particular, the model proposes a mathematical framework in which egocentric vectors representing distance to features is coded by synaptically induced theta waves. It is proposed that individual dendrites cause phase shifts of theta waves that correspond to different affine transformations in different individual neurons. The exact dendritic mechanism of this model are not clear, but could guide more detailed biophysical simulations of dendritic dynamics mediated by *h* current and potassium currents to understand both the encoding of sensitivity to specific dynamics and the potential for systematic phase shifts in entorhinal neurons that code the spatial phase of individual grid cells.

ACKNOWLEDGMENTS

This work supported by the National Institutes of Health, grant numbers R01 MH120073, R01 MH60013 (to Michael E. Hasselmo), F32 NS101836 (to Andrew S. Alexander) and by the Office of Naval Research MURI N00014-16-1-2832 (to Michael E. Hasselmo) and MURI N00014-19-1-2571 and DURIP N00014-17-1-2304. Model in Figures 4–7 created and simulated by MEH.

CONFLICT OF INTEREST STATEMENT

The authors declare no conflicts of interest.

DATA AVAILABILITY STATEMENT

Data available on request from the authors.

ORCID

Michael E. Hasselmo https://orcid.org/0000-0002-9925-6377

REFERENCES

Ainge, J. A., van der Meer, M. A., Langston, R. F., & Wood, E. R. (2007). Exploring the role of context-dependent hippocampal activity in spatial alternation behavior. *Hippocampus*, *17*, 988–1002.

Alexander, A. S., Carstensen, L. C., Hinman, J. R., Raudies, F., Chapman, G. W., & Hasselmo, M. E. (2020). Egocentric boundary vector tuning of the retrosplenial cortex. *Science Advances*, *6*, eaaz2322.

Alexander, A. S., & Nitz, D. A. (2015). Retrosplenial cortex maps the conjunction of internal and external spaces. *Nature Neuroscience*, *18*, 1143–1151.

Alexander, A. S., & Nitz, D. A. (2017). Spatially periodic activation patterns of retrosplenial cortex encode route sub-spaces and distance traveled. *Current Biology: CB*, *27*, 1551–1560.

Alexander, A. S., Rangel, L. M., Tingley, D., & Nitz, D. A. (2018). Neurophysiological signatures of temporal coordination between retrosplenial cortex and the hippocampal formation. *Behavioral Neuroscience*, *132*, 453–468.

Alexander, A. S., Tung, J. C., Chapman, G. W., Conner, A. M., Shelley, L. E., Hasselmo, M. E., & Nitz, D. A. (2022). Adaptive integration of self-motion and goals in posterior parietal cortex. *Cell Reports*, *38*, 110504.

Alonso, A., & Kohler, C. (1984). A study of the reciprocal connections between the septum and the entorhinal area using anterograde and retrograde axonal transport methods in the rat brain. *The Journal of Comparative Neurology*, *225*, 327–343.

Andersen, R. A., Essick, G. K., & Siegel, R. M. (1985). Encoding of spatial location by posterior parietal neurons. *Science (New York, N.Y.)*, *230*, 456–458.

Anderson, M. I., & Jeffery, K. J. (2003). Heterogeneous modulation of place cell firing by changes in context. *The Journal of Neuroscience*, *23*, 8827–8835.

Barry, C., Hayman, R., Burgess, N., & Jeffery, K. J. (2007). Experience-dependent rescaling of entorhinal grids. *Nature Neuroscience*, *10*, 682–684.

Barry, C., Lever, C., Hayman, R., Hartley, T., Burton, S., O'Keefe, J., Jeffery, K., & Burgess, N. (2006). The boundary vector cell model of place cell firing and spatial memory. *Reviews in the Neurosciences*, *17*, 71–97.

Bicanski, A., & Burgess, N. (2018). A neural-level model of spatial memory and imagery. *eLife*, *7*, e33752.

Bicanski, A., & Burgess, N. (2019). A computational model of visual recognition memory via grid cells. *Current Biology*, *29*(979–990), e974.

Bicanski, A., & Burgess, N. (2020). Neuronal vector coding in spatial cognition. *Nature Reviews. Neuroscience*, *21*, 453–470.

Boehlen, A., Heinemann, U., & Erchova, I. (2010). The range of intrinsic frequencies represented by medial entorhinal cortex stellate cells extends with age. *The Journal of Neuroscience*, *30*, 4585–4589.

Bonnevie, T., Dunn, B., Fyhn, M., Hafting, T., Derdikman, D., Kubie, J. L., Roudi, Y., Moser, E. I., & Moser, M. B. (2013). Grid cells require excitatory drive from the hippocampus. *Nature Neuroscience*, *16*, 309–317.

Brandon, M. P., Bogaard, A. R., Libby, C. P., Connerney, M. A., Gupta, K., & Hasselmo, M. E. (2011). Reduction of theta rhythm dissociates grid cell spatial periodicity from directional tuning. *Science*, *332*, 595–599.

Brandon, M. P., Koenig, J., & Leutgeb, S. (2014). Parallel and convergent processing in grid cell, head-direction cell, boundary cell, and place cell networks. *Wiley Interdisciplinary Reviews: Cognitive Science*, *5*, 207–219.

Brazhnik, E. S., & Fox, S. E. (1999). Action potentials and relations to the theta rhythm of medial septal neurons in vivo. *Experimental Brain Research*, *127*, 244–258.

Brown, E. N., Frank, L. M., Tang, D., Quirk, M. C., & Wilson, M. A. (1998). A statistical paradigm for neural spike train decoding applied to position prediction from ensemble firing patterns of rat hippocampal place cells. *The Journal of Neuroscience*, *18*, 7411–7425.

Brown, M. A., & Sharp, P. E. (1995). Simulation of spatial learning in the Morris water maze by a neural network model of the hippocampal formation and nucleus accumbens. *Hippocampus*, *5*, 171–188.

Burak, Y., & Fiete, I. R. (2009). Accurate path integration in continuous attractor network models of grid cells. *PLoS Computational Biology*, *5*, e1000291.

Burgess, N. (2008). Grid cells and theta as oscillatory interference: Theory and predictions. *Hippocampus*, *18*, 1157–1174.

Burgess, N., Barry, C., & O'Keefe, J. (2007). An oscillatory interference model of grid cell firing. *Hippocampus*, *17*, 801–812.

Burgess, N., Becker, S., King, J. A., & O'Keefe, J. (2001). Memory for events and their spatial context: Models and experiments. *Philosophical Transactions of the Royal Society of London. Series B, Biological Sciences*, *356*, 1493–1503.

Burgess, N., Jackson, A., Hartley, T., & O'Keefe, J. (2000). Predictions derived from modelling the hippocampal role in navigation. *Biological Cybernetics*, *83*, 301–312.

Burgess, N., & O'Keefe, J. (1996). Neuronal computations underlying the firing of place cells and their role in navigation. *Hippocampus*, *6*, 749–762.

Bush, D., Bisby, J. A., Bird, C. M., Gollwitzer, S., Rodionov, R., Diehl, B., McEvoy, A. W., Walker, M. C., & Burgess, N. (2017). Human hippocampal theta power indicates movement onset and distance travelled. *Proceedings of the National Academy of Sciences of the United States of America*, *114*, 12297–12302.

Bush, D., & Burgess, N. (2014). A hybrid oscillatory interference/continuous attractor network model of grid cell firing. *The Journal of Neuroscience*, *34*, 5065–5079.

Buzsaki, G. (2002). Theta oscillations in the hippocampus. *Neuron*, *33*, 325–340.

Byrne, P., Becker, S., & Burgess, N. (2007). Remembering the past and imagining the future: A neural model of spatial memory and imagery. *Psychological Review*, *114*, 340–375.

Caggiano, V., Fogassi, L., Rizzolatti, G., Thier, P., & Casile, A. (2009). Mirror neurons differentially encode the peripersonal and extrapersonal space of monkeys. *Science*, *324*, 403–406.

Caplan, J. B., Madsen, J. R., Schulze-Bonhage, A., Aschenbrenner-Scheibe, R., Newman, E. L., & Kahana, M. J. (2003). Human theta oscillations related to sensorimotor integration and spatial learning. *The Journal of Neuroscience*, *23*, 4726–4736.

Carpenter, F., Burgess, N., & Barry, C. (2017). Modulating medial septal cholinergic activity reduces medial entorhinal theta frequency without affecting speed or grid coding. *Scientific Reports*, *7*, 14573.

Carstensen, L. C., Alexander, A. S., Chapman, G. W., Lee, A., & Hasselmo, M. E. (2021). Neural responses in retrosplenial cortex associated with environmental alterations. *iScience*, *24*, 103377.

Chen, G., Manson, D., Cacucci, F., & Wills, T. J. (2016). Absence of visual input results in the disruption of grid cell firing in the mouse. *Current Biology*, *26*, 2335–2342.

Chen, L. L., Lin, L. H., Barnes, C. A., & McNaughton, B. L. (1994). Head-direction cells in the rat posterior cortex. II. Contributions of visual and ideothetic information to the directional firing. *Experimental Brain Research*, *101*, 24–34.

Chen, L. L., Lin, L. H., Green, E. J., Barnes, C. A., & McNaughton, B. L. (1994). Head-direction cells in the rat posterior cortex. I. Anatomical distribution and behavioral modulation. *Experimental Brain Research*, *101*, 8–23.

Cho, J., & Sharp, P. E. (2001). Head direction, place, and movement correlates for cells in the rat retrosplenial cortex. *Behavioral Neuroscience*, *115*, 3–25.

Chollet, F. (2019). On the measure of intelligence. *ArXiv*, *1911*, 01547.

Chrastil, E. R., Sherrill, K. R., Hasselmo, M. E., & Stern, C. E. (2015). There and back again: Hippocampus and retrosplenial cortex track homing distance during human path integration. *The Journal of Neuroscience*, *35*, 15442–15452.

Chrastil, E. R., Sherrill, K. R., Hasselmo, M. E., & Stern, C. E. (2016). Which way and how far? Tracking of translation and rotation information for human path integration. *Human Brain Mapping*, *37*, 3636–3655.

Chrastil, E. R., Tobyne, S. M., Nauer, R. K., Chang, A. E., & Stern, C. E. (2018). Converging meta-analytic and connectomic evidence for functional subregions within the human retrosplenial region. *Behavioral Neuroscience*, *132*, 339–355.

Climer, J. R., Newman, E. L., & Hasselmo, M. E. (2013). Phase coding by grid cells in unconstrained environments: Two-dimensional phase precession. *The European Journal of Neuroscience*, *38*, 2526–2541.

Colom, L. V., Castaneda, M. T., Reyna, T., Hernandez, S., & Garrido-sanabria, E. (2005). Characterization of medial septal glutamatergic neurons and their projection to the hippocampus. *Synapse*, *58*, 151–164.

Dannenberg, H., Kelley, C., Hoyland, A., Monaghan, C. K., & Hasselmo, M. E. (2019). The firing rate speed code of entorhinal speed cells differs across behaviorally relevant time scales and does not depend on medial septum inputs. *The Journal of Neuroscience*, *39*, 3434–3453.

Dannenberg, H., Lazaro, H., Nambiar, P., Hoyland, A., & Hasselmo, M. E. (2020). Effects of visual inputs on neural dynamics for coding of location and running speed in medial entorhinal cortex. *eLife*, *9*, e62500.

Derdikman, D., Whitlock, J. R., Tsao, A., Fyhn, M., Hafting, T., Moser, M. B., & Moser, E. I. (2009). Fragmentation of grid cell maps in a multicompartment environment. *Nature Neuroscience*, *12*, 1325–1332.

Deshmukh, S. S., & Knierim, J. J. (2011). Representation of non-spatial and spatial information in the lateral entorhinal cortex. *Frontiers in Behavioral Neuroscience*, *5*, 69.

Deshmukh, S. S., & Knierim, J. J. (2013). *Influence of local objects on hippocampal representations: Landmark vectors and memory*. Hippocampus.

Deshmukh, S. S., Yoganarasimha, D., Voicu, H., & Knierim, J. J. (2010). Theta modulation in the medial and the lateral entorhinal cortices. *Journal of Neurophysiology*, *104*, 994–1006.

Dickson, C. T., Magistretti, J., Shalinsky, M. H., Fransen, E., Hasselmo, M. E., & Alonso, A. (2000). Properties and role of I(h) in the pacing of subthreshold oscillations in entorhinal cortex layer II neurons. *Journal of Neurophysiology*, *83*, 2562–2579.

Diehl, G. W., Hon, O. J., Leutgeb, S., & Leutgeb, J. K. (2017). Grid and nongrid cells in medial entorhinal cortex represent spatial location and environmental features with complementary coding schemes. *Neuron*, *94*(83–92), e86.

Do, Q., Hasselmo, M. E. (2021). Neural circuits and symbolic processing. *Neurobiology of Learning and Memory*, *186*, 107552.

Dodson, P. D., Pastoll, H., & Nolan, M. F. (2011). Dorsal-ventral organization of theta-like activity intrinsic to entorhinal stellate neurons is mediated by differences in stochastic current fluctuations. *The Journal of Physiology*, *589*, 2993–3008.

Doeller, C. F., Barry, C., & Burgess, N. (2010). Evidence for grid cells in a human memory network. *Nature*, *463*, 657–661.

Domnisoru, C., Kinkhabwala, A. A., & Tank, D. W. (2013). Membrane potential dynamics of grid cells. *Nature*, *495*, 199–204.

Douchamps, V., Jeewajee, A., Blundell, P., Burgess, N., & Lever, C. (2013). Evidence for encoding versus retrieval scheduling in the hippocampus by theta phase and acetylcholine. *The Journal of Neuroscience*, *33*, 8689–8704.

Eichenbaum, H. (2017). The role of the hippocampus in navigation is memory. *Journal of Neurophysiology*, *117*, 1785–1796.

Eichenbaum, H., Stewart, C., & Morris, R. G. (1990). Hippocampal representation in place learning. *The Journal of Neuroscience*, *10*, 3531–3542.

Ekstrom, A. D., Caplan, J. B., Ho, E., Shattuck, K., Fried, I., & Kahana, M. J. (2005). Human hippocampal theta activity during virtual navigation. *Hippocampus*, *15*, 881–889.

Ekstrom, A. D., Kahana, M. J., Caplan, J. B., Fields, T. A., Isham, E. A., Newman, E. L., & Fried, I. (2003). Cellular networks underlying human spatial navigation. *Nature*, *425*, 184–188.

Epstein, R. A., & Higgins, J. S. (2007). Differential parahippocampal and retrosplenial involvement in three types of visual scene recognition. *Cerebral Cortex*, *17*, 1680–1693.

Epstein, R. A., Parker, W. E., & Feiler, A. M. (2007). Where am I now? Distinct roles for parahippocampal and retrosplenial cortices in place recognition. *The Journal of Neuroscience*, *27*, 6141–6149.

Erchova, I., Kreck, G., Heinemann, U., & Herz, A. V. (2004). Dynamics of rat entorhinal cortex layer II and III cells: Characteristics of membrane potential resonance at rest predict oscillation properties near threshold. *The Journal of Physiology*, *560*, 89–110.

Erdem, U. M., & Hasselmo, M. (2012). A goal-directed spatial navigation model using forward trajectory planning based on grid cells. *The European Journal of Neuroscience*, *35*, 916–931.

Erdem, U. M., & Hasselmo, M. E. (2014). A biologically inspired hierarchical goal directed navigation model. *Journal of Physiology*, *Paris*, *108*, 28–37.

Feng, T., Silva, D., & Foster, D. J. (2015). Dissociation between the experience-dependent development of hippocampal theta sequences and single-trial phase precession. *The Journal of Neuroscience*, *35*, 4890–4902.

Fenton, A. A., Kao, H. Y., Neymotin, S. A., Olypher, A., Vayntrub, Y., Lytton, W. W., & Ludvig, N. (2008). Unmasking the CA1 ensemble place code by exposures to small and large environments: More place cells and multiple, irregularly arranged, and expanded place fields in the larger space. *The Journal of Neuroscience*, *28*, 11250–11262.

Fenton, A. A., & Muller, R. U. (1998). Place cell discharge is extremely variable during individual passes of the rat through the firing field. *Proceedings of the National Academy Sciences of the United States of America*, *95*, 3182–3187.

Ferbinteanu, J., & Shapiro, M. L. (2003). Prospective and retrospective memory coding in the hippocampus. *Neuron*, *40*, 1227–1239.

Ferrante, M., Shay, C. F., Tsuno, Y., Chapman, G. W., & Hasselmo, M. E. (2017). Post-inhibitory rebound spikes in rat medial entorhinal layer II/III principal cells: In vivo, in vitro, and computational modeling characterization. *Cerebral Cortex*, *27*(3), 2111–2125.

Fischer, L. F., Mojica Soto-Albors, R., Buck, F., & Harnett, M. T. (2020). Representation of visual landmarks in retrosplenial cortex. *eLife*, *9*, e51548.

Foster, D. J., & Wilson, M. A. (2007). Hippocampal theta sequences. *Hippocampus*, *17*, 1093–1099.

Fox, S. E., Wolfson, S., & Ranck, J. B., Jr. (1986). Hippocampal theta rhythm and the firing of neurons in walking and urethane anesthetized rats. *Brain Research*, *62*, 495–508.

Fransen, E., Alonso, A. A., Dickson, C. T., Magistretti, J., & Hasselmo, M. E. (2004). Ionic mechanisms in the generation of subthreshold oscillations and action potential clustering in entorhinal layer II stellate neurons. *Hippocampus*, *14*, 368–384.

Fuhrmann, F., Justus, D., Sosulina, L., Kaneko, H., Beutel, T., Friedrichs, D., Schoch, S., Schwarz, M. K., Fuhrmann, M., & Remy, S. (2015). Locomotion, theta oscillations, and the speed-correlated firing of hippocampal neurons are controlled by a medial septal glutamatergic circuit. *Neuron*, *86*, 1253–1264.

Fuhs, M. C., & Touretzky, D. S. (2006). A spin glass model of path integration in rat medial entorhinal cortex. *The Journal of Neuroscience*, *26*, 4266–4276.

Fyhn, M., Hafting, T., Treves, A., Moser, M. B., & Moser, E. I. (2007). Hippocampal remapping and grid realignment in entorhinal cortex. *Nature*, *446*, 190–194.

Garden, D. L., Dodson, P. D., O'Donnell, C., White, M. D., & Nolan, M. F. (2008). Tuning of synaptic integration in the medial entorhinal cortex to the organization of grid cell firing fields. *Neuron*, *60*, 875–889.

Georges-Francois, P., Rolls, E. T., & Robertson, R. G. (1999). Spatial view cells in the primate hippocampus: Allocentric view not head direction or eye position or place. *Cerebral Cortex*, *9*, 197–212.

Georgopoulos, A. P. (1987). Cortical mechanisms subserving reaching. *Ciba Foundation Symposium*, *132*, 125–141.

Giocomo, L. M., & Hasselmo, M. E. (2008). Time constants of h current in layer ii stellate cells differ along the dorsal to ventral axis of medial entorhinal cortex. *The Journal of Neuroscience*, *28*, 9414–9425.

Giocomo, L. M., & Hasselmo, M. E. (2009). Knock-out of HCN1 subunit flattens dorsal-ventral frequency gradient of medial entorhinal neurons in adult mice. *The Journal of Neuroscience*, *29*, 7625–7630.

Giocomo, L. M., Hussaini, S. A., Zheng, F., Kandel, E. R., Moser, M. B., & Moser, E. I. (2011). Grid cells use HCN1 channels for spatial scaling. *Cell*, *147*, 1159–1170.

Giocomo, L. M., Zilli, E. A., Fransen, E., & Hasselmo, M. E. (2007). Temporal frequency of subthreshold oscillations scales with entorhinal grid cell field spacing. *Science*, *315*, 1719–1722.

Givens, B. (1996). Stimulus-evoked resetting of the dentate theta rhythm: Relation to working memory. *Neuroreport*, *8*, 159–163.

Gofman, X., Tocker, G., Weiss, S., Boccara, C. N., Lu, L., Moser, M. B., Moser, E. I., Morris, G., & Derdikman, D. (2019). Dissociation between postrhinal cortex and downstream parahippocampal regions in the representation of egocentric boundaries. *Current Biology*, *29*(2751–2757), e2754.

Gothard, K. M., Skaggs, W. E., & McNaughton, B. L. (1996). Dynamics of mismatch correction in the hippocampal ensemble code for space: Interaction between path integration and environmental cues. *The Journal of Neuroscience*, *16*, 8027–8040.

Gothard, K. M., Skaggs, W. E., Moore, K. M., & McNaughton, B. L. (1996). Binding of hippocampal CA1 neural activity to multiple reference frames in a landmark-based navigation task. *The Journal of Neuroscience*, *16*, 823–835.

Guanella, A., Kiper, D., & Verschure, P. (2007). A model of grid cells based on a twisted torus topology. *International Journal of Neural Systems*, *17*, 231–240.

Guise, K. G., & Shapiro, M. L. (2017). Medial prefrontal cortex reduces memory interference by modifying hippocampal encoding. *Neuron*, *94*(183–192), e188.

Gupta, K., Beer, N. J., Keller, L. A., & Hasselmo, M. E. (2014). Medial entorhinal grid cells and head direction cells rotate with a T-maze more often during less recently experienced rotations. *Cerebral Cortex*, *24*, 1630–1644.

Haas, J. S., Dorval, A. D., 2nd, & White, J. A. (2007). Contributions of Ih to feature selectivity in layer II stellate cells of the entorhinal cortex. *Journal of Computational Neuroscience*, *22*, 161–171.

Haas, J. S., & White, J. A. (2002). Frequency selectivity of layer II stellate cells in the medial entorhinal cortex. *Journal of Neurophysiology*, *88*, 2422–2429.

Hafting, T., Fyhn, M., Bonnevie, T., Moser, M. B., & Moser, E. I. (2008). Hippocampus-independent phase precession in entorhinal grid cells. *Nature*, *453*, 1248–1252.

Hafting, T., Fyhn, M., Molden, S., Moser, M.-B., & Moser, E. I. (2005). Microstructure of a spatial map in the entorhinal cortex. *Nature*, *436*, 801–806.

Hardcastle, K., Ganguli, S., & Giocomo, L. M. (2015). Environmental boundaries as an error correction mechanism for grid cells. *Neuron*, *86*, 827–839.

Hardcastle, K., Maheswaranathan, N., Ganguli, S., & Giocomo, L. M. (2017). A multiplexed, heterogeneous, and adaptive code for navigation in medial entorhinal cortex. *Neuron*, *94*, 375–387.

Harootonian, S. K., Ekstrom, A. D., & Wilson, R. C. (2022). Combination and competition between path integration and landmark navigation in the estimation of heading direction. *PLoS Computational Biology*, *18*, e1009222.

Hartley, T., Burgess, N., Lever, C., Cacucci, F., & O'Keefe, J. (2000). Modeling place fields in terms of the cortical inputs to the hippocampus. *Hippocampus*, *10*, 369–379.

Hartley, T., Lever, C., Burgess, N., & O'Keefe, J. (2014). Space in the brain: How the hippocampal formation supports spatial cognition. *Philosophical Transactions of the Royal Society of London. Series B, Biological Sciences*, *369*, 20120510.

Harvey, C. D., Collman, F., Dombeck, D. A., & Tank, D. W. (2009). Intracellular dynamics of hippocampal place cells during virtual navigation. *Nature*, *461*, 941–946.

Hasselmo, M. E. (2008). Grid cell mechanisms and function: Contributions of entorhinal persistent spiking and phase resetting. *Hippocampus*, *18*, 1213–1229.

Hasselmo, M. E. (2009). A model of episodic memory: Mental time travel along encoded trajectories using grid cells. *Neurobiology of Learning and Memory*, *92*, 559–573.

Hasselmo, M. E., Alexander, A. S., Hoyland, A., Robinson, J. C., Bezaire, M. J., Chapman, G. W., Saudargiene, A., Carstensen, L. C., & Dannenberg, H. (2021). The unexplored territory of neural models: Potential guides for exploring the function of metabotropic neuromodulation. *Neuroscience*, *456*, 143–158.

Hasselmo, M. E., Bodelón, C., & Wyble, B. P. (2002). A proposed function for hippocampal theta rhythm: Separate phases of encoding and retrieval enhance reversal of prior learning. *Neural Computation*, *14*, 793–817.

Hasselmo, M. E., & Eichenbaum, H. (2005). Hippocampal mechanisms for the context-dependent retrieval of episodes. *Neural Networks*, *18*, 1172–1190.

Hasselmo, M. E., & Shay, C. F. (2014). Grid cell firing patterns may arise from feedback interaction between intrinsic rebound spiking and transverse traveling waves with multiple heading angles. *Frontiers in Systems Neuroscience*, *8*, 201.

He, Q., & Brown, T. I. (2019). Environmental barriers disrupt grid-like representations in humans during navigation. *Current Biology*, *29*(2718–2722), e2713.

Heys, J. G., Giocomo, L. M., & Hasselmo, M. E. (2010). Cholinergic modulation of the resonance properties of stellate cells in layer II of medial entorhinal cortex. *Journal of Neurophysiology*, *104*, 258–270.

Heys, J. G., Rangarajan, K. V., & Dombeck, D. A. (2014). The functional micro-organization of grid cells revealed by cellular-resolution imaging. *Neuron*, *84*, 1079–1090.

Hinman, J. R., Brandon, M. P., Climer, J. R., Chapman, G. W., & Hasselmo, M. E. (2016). Multiple running speed signals in medial entorhinal cortex. *Neuron*, *91*, 666–679.

Hinman, J. R., Chapman, G. W., & Hasselmo, M. E. (2019). Neuronal representation of environmental boundaries in egocentric coordinates. *Nature Communications*, *10*, 2772.

Hoffman, K. L., Dragan, M. C., Leonard, T. K., Micheli, C., Montefusco-Siegmund, R., & Valiante, T. A. (2013). Saccades during visual exploration align hippocampal 3-8 Hz rhythms in human and non-human primates. *Frontiers in Systems Neuroscience*, *7*, 43.

Hoydal, O. A., Skytoen, E. R., Andersson, S. O., Moser, M. B., & Moser, E. I. (2019). Object-vector coding in the medial entorhinal cortex. *Nature*, *568*, 400–404.

Huxter, J. R., Senior, T. J., Allen, K., & Csicsvari, J. (2008). Theta phase-specific codes for two-dimensional position, trajectory and heading in the hippocampus. *Nature Neuroscience*, *11*, 587–594.

Hyman, J. M., Wyble, B. P., Goyal, V., Rossi, C. A., & Hasselmo, M. E. (2003). Stimulation in hippocampal region CA1 in behaving rats yields long-term potentiation when delivered to the peak of theta and long-term depression when delivered to the trough. *The Journal of Neuroscience*, *23*, 11725–11731.

Jacob, P.-Y., Casali, G., Spieser, L., Page, H., Overington, D., & Jeffery, K. (2017). An independent, landmark-dominated head-direction signal in dysgranular retrosplenial cortex. *Nature Neuroscience*, *20*, 173–175.

Jacobs, J., Weidemann, C. T., Miller, J. F., Solway, A., Burke, J. F., Wei, X. X., Suthana, N., Sperling, M. R., Sharan, A. D., Fried, I., & Kahana, M. J. (2013). Direct recordings of grid-like neuronal activity in human spatial navigation. *Nature Neuroscience*, *16*, 1188–1190.

Jeewajee, A., Barry, C., Douchamps, V., Manson, D., Lever, C., & Burgess, N. (2014). Theta phase precession of grid and place cell firing in open environments. *Philosophical Transactions of the Royal Society of London. Series B, Biological Sciences*, *369*, 20120532.

Jeewajee, A., Barry, C., O'Keefe, J., & Burgess, N. (2008). Grid cells and theta as oscillatory interference: Electrophysiological data from freely moving rats. *Hippocampus*, *18*, 1175–1185.

Jeffery, K. J., Donnett, J. G., & O'Keefe, J. (1995). Medial septal control of theta-correlated unit firing in the entorhinal cortex of awake rats. *Neuroreport*, *6*, 2166–2170.

Jutras, M. J., & Buffalo, E. A. (2014). Oscillatory correlates of memory in non-human primates. *NeuroImage*, *85*(Pt 2), 694–701.

Jutras, M. J., Fries, P., & Buffalo, E. A. (2013). Oscillatory activity in the monkey hippocampus during visual exploration and memory formation. *Proceedings of the National Academy of Sciences of the United States of America*, *110*, 13144–13149.

Kalaska, J. F., Caminiti, R., & Georgopoulos, A. P. (1983). Cortical mechanisms related to the direction of two-dimensional arm movements: Relations in parietal area 5 and comparison with motor cortex. *Experimental Brain Research*, *51*, 247–260.

Katz, C. N., Schjetnan, A. G. P., Patel, K., Barkley, V., Hoffman, K. L., Kalia, S. K., Duncan, K. D., & Valiante, T. A. (2022). A corollary discharge mediates saccade-related inhibition of single units in mnemonic structures of the human brain. *Current Biology*, *32*(3082–3094), e3084.

Killian, N. J., & Buffalo, E. A. (2018). Grid cells map the visual world. *Nature Neuroscience*, *21*, 161–162.

Killian, N. J., Jutras, M. J., & Buffalo, E. A. (2012). A map of visual space in the primate entorhinal cortex. *Nature*, *491*, 761–764.

Kinsky, N. R., Mau, W., Sullivan, D. W., Levy, S. J., Ruesch, E. A., & Hasselmo, M. E. (2020). Trajectory-modulated hippocampal neurons persist throughout memory-guided navigation. *Nature Communications*, *11*, 2443.

Koenig, J., Linder, A. N., Leutgeb, J. K., & Leutgeb, S. (2011). The spatial periodicity of grid cells is not sustained during reduced theta oscillations. *Science*, *332*, 592–595.

Köhler, C., Chan-Palay, V., & Wu, J. Y. (1984). Septal neurons containing glutamic acid decarboxylase immunoreactivity project to the hippocampal region in the rat brain. *Anatomy and Embryology*, *169*, 41–44.

Koike, B. D. V., Farias, K. S., Billwiller, F., Almeida-Filho, D., Libourel, P. A., Tiran-Cappello, A., Parmentier, R., Blanco, W., Ribeiro, S., Luppi, P. H., & Queiroz, C. M. (2017). Electrophysiological evidence that the Retrosplenial cortex displays a strong and specific activation phased with hippocampal theta during paradoxical (REM) sleep. *The Journal of Neuroscience*, *37*, 8003–8013.

Kropff, E., Carmichael, J. E., Moser, M. B., & Moser, E. I. (2015). Speed cells in the medial entorhinal cortex. *Nature*, *523*, 419–424.

Kropff, E., & Treves, A. (2008). The emergence of grid cells: Intelligent design or just adaptation? *Hippocampus*, *18*, 1256–1269.

Kunda, M., McGreggor, K., & Goel, A. K. (2013). A computational model for solving problems from the Raven's progressive matrices intelligence test using iconic visual representations. *Cognitive Systems Research*, *22-23*, 47–66.

LaChance, P. A., Graham, J., Shapiro, B. L., Morris, A. J., & Taube, J. S. (2022). Landmark-modulated directional coding in postrhinal cortex. *Science Advances*, *8*, eabg8404.

LaChance, P. A., & Taube, J. S. (2022). A model for transforming egocentric views into goal-directed behavior. *Hippocampus*, *this volume*.

LaChance, P. A., Todd, T. P., & Taube, J. S. (2019). A sense of space in postrhinal cortex. *Science*, *365*, eaax4192.

Lancaster, B., Hu, H., Gibb, B., & Storm, J. F. (2006). Kinetics of ion channel modulation by cAMP in rat hippocampal neurones. *The Journal of Physiology*, *576*, 403–417.

Lepperod, M. E., Christensen, A. C., Lensjo, K. K., Buccino, A. P., Yu, J., Fyhn, M., & Hafting, T. (2021). Optogenetic pacing of medial septum parvalbumin-positive cells disrupts temporal but not spatial firing in grid cells. *Science Advances*, *7*, eabd5684.

Leung, L. W., & Yim, C. Y. (1986). Intracellular records of theta rhythm in hippocampal CA1 cells of the rat. *Brain Research*, *367*, 323–327.

Lever, C., Burton, S., Jeewajee, A., O'Keefe, J., & Burgess, N. (2009). Boundary vector cells in the subiculum of the hippocampal formation. *The Journal of Neuroscience*, *29*, 9771–9777.

Lever, C., Wills, T., Cacucci, F., Burgess, N., & O'Keefe, J. (2002). Long-term plasticity in hippocampal place-cell representation of environmental geometry. *Nature*, *416*, 90–94.

Lewis, M., Purdy, S., Ahmad, S., & Hawkins, J. (2019). Locations in the neocortex: A theory of sensorimotor object recognition using cortical grid cells. *Frontiers in Neural Circuits*, *13*, 22.

Lian, Y., & Burkitt, A. N. (2021). Learning an efficient hippocampal place map from entorhinal inputs using non-negative sparse coding. *eNeuro*, *8*, *ENEURO.0557-20.2021*.

Lian, Y., Williams, S., Alexander, A. S., Hasselmo, M. E., & Burkitt, A. N. (2022). Learning the vector coding of egocentric boundary cells from visual data. *BioRXiv in Review*.

Ludvig, N., Tang, H. M., Gohil, B. C., & Botero, J. M. (2004). Detecting location-specific neuronal firing rate increases in the hippocampus of freely-moving monkeys. *Brain Research*, *1014*, 97–109.

Maidenbaum, S., Miller, J., Stein, J. M., & Jacobs, J. (2018). Grid-like hexadirectional modulation of human entorhinal theta oscillations. *Proceedings of the National Academy of Sciences of the United States of America*, *115*, 10798–10803.

Manns, J. R., Zilli, E. A., Ong, K. C., Hasselmo, M. E., & Eichenbaum, H. (2007). Hippocampal CA1 spiking during encoding and retrieval: Relation to theta phase. *Neurobiology of Learning and Memory*, *87*, 9–20.

Manseau, F., Goutagny, R., Danik, M., & Williams, S. (2008). The hippocamposeptal pathway generates rhythmic firing of GABAergic neurons in the medial septum and diagonal bands: An investigation using a complete septohippocampal preparation in vitro. *The Journal of Neuroscience*, *28*, 4096–4107.

Mao, D., Avila, E., Caziot, B., Laurens, J., Dickman, J. D., & Angelaki, D. E. (2021). Spatial modulation of hippocampal activity in freely moving macaques. *Neuron*, *109*(3521–3534), e3526.

Mao, D., Kandler, S., McNaughton, B. L., & Bonin, V. (2017). Sparse orthogonal population representation of spatial context in the retrosplenial cortex. *Nature Communications*, *8*, 243.

Mao, D., Molina, L. A., Bonin, V., & McNaughton, B. L. (2020). Vision and locomotion combine to drive path integration sequences in mouse Retrosplenial cortex. *Current Biology*, *30*(1680–1688), e1684.

Mao, D., Neumann, A. R., Sun, J., Bonin, V., Mohajerani, M. H., & McNaughton, B. L. (2018). Hippocampus-dependent emergence of spatial sequence coding in retrosplenial cortex. *Proceedings of the National Academy of Sciences of the United States of America*, *115*, 8015–8018.

Maurer, A. P., Cowen, S. L., Burke, S. N., Barnes, C. A., & McNaughton, B. L. (2006). Phase precession in hippocampal interneurons showing strong functional coupling to individual pyramidal cells. *The Journal of Neuroscience*, *26*, 13485–13492.

McCartney, H., Johnson, A. D., Weil, Z. M., & Givens, B. (2004). Theta reset produces optimal conditions for long-term potentiation. *Hippocampus*, *14*, 684–687.

McNaughton, B. L., Barnes, C. A., Gerrard, J. L., Gothard, K., Jung, M. W., Knierim, J. J., Kudrimoti, H., Qin, Y., Skaggs, W. E., Suster, M., & Weaver, K. L. (1996). Deciphering the hippocampal polyglot: The hippocampus as a path integration system. *The Journal of Experimental Biology*, *199*, 173–185.

McNaughton, B. L., Barnes, C. A., & O'Keefe, J. (1983). The contributions of position, direction, and velocity to single unit-activity in the hippocampus of freely-moving rats. *Experimental Brain Research*, *52*, 41–49.

McNaughton, B. L., Battaglia, F. P., Jensen, O., Moser, E. I., & Moser, M. B. (2006). Path integration and the neural basis of the 'cognitive map'. *Nature Reviews. Neuroscience*, *7*, 663–678.

Meister, M. L. R., & Buffalo, E. A. (2018). Neurons in primate entorhinal cortex represent gaze position in multiple spatial reference frames. *The Journal of Neuroscience*, *38*, 2430–2441.

Mel, B. W. (1993). Synaptic integration in an excitable dendritic tree. *Journal of Neurophysiology*, *70*, 1086–1101.

Miller, J. F., Neufang, M., Solway, A., Brandt, A., Trippel, M., Mader, I., Hefft, S., Merkow, M., Polyn, S. M., Jacobs, J., Kahana, M. J., & Schulze-Bonhage, A. (2013). Neural activity in human hippocampal formation reveals the spatial context of retrieved memories. *Science*, *342*, 1111–1114.

Mitchell, S. J., Rawlins, J. N., Steward, O., & Olton, D. S. (1982). Medial septal area lesions disrupt theta rhythm and cholinergic staining in medial entorhinal cortex and produce impaired radial arm maze behavior in rats. *The Journal of Neuroscience*, *2*, 292–302.

Morris, R. G., Garrud, P., Rawlins, J. N., & O'Keefe, J. (1982). Place navigation impaired in rats with hippocampal lesions. *Nature*, *297*, 681–683.

Mountcastle, V. B., Lynch, J. C., Georgopoulos, A., Sakata, H., & Acuna, C. (1975). Posterior parietal association cortex of the monkey: Command functions for operations within extrapersonal space. *Journal of Neurophysiology*, *38*, 871–908.

Muller, R. U., & Kubie, J. L. (1987). The effects of changes in the environment on the spatial firing of hippocampal complex-spike cells. *The Journal of Neuroscience*, *7*, 1951–1968.

Muller, R. U., Kubie, J. L., & Ranck, J. B., Jr. (1987). Spatial firing patterns of hippocampal complex-spike cells in a fixed environment. *The Journal of Neuroscience*, *7*, 1935–1950.

Munn, R. G. K., Mallory, C. S., Hardcastle, K., Chetkovich, D. M., & Giocomo, L. M. (2020). Entorhinal velocity signals reflect environmental geometry. *Nature Neuroscience*, *23*, 239–251.

Nadasdy, Z., Howell, D. H. P., Torok, A., Nguyen, T. P., Shen, J. Y., Briggs, D. E., Modur, P. N., & Buchanan, R. J. (2022). Phase coding of spatial representations in the human entorhinal cortex. *Science Advances*, *8*, eabm6081.

Nadasdy, Z., Nguyen, T. P., Torok, A., Shen, J. Y., Briggs, D. E., Modur, P. N., & Buchanan, R. J. (2017). Context-dependent spatially periodic activity in the human entorhinal cortex. *Proceedings of the National Academy of Sciences of the United States of America*, *114*, E3516–E3525.

Newman, E. L., & Hasselmo, M. E. (2014). Grid cell firing properties vary as a function of theta phase locking preferences in the rat medial entorhinal cortex. *Frontiers in Systems Neuroscience*, *8*, 193.

Ning, W., Bladon, J. H., & Hasselmo, M. E. (2022). Complementary representations of time in the prefrontal cortex and hippocampus. *Hippocampus*, *32*, 577–596.

Nitz, D. (2009). Parietal cortex, navigation, and the construction of arbitrary reference frames for spatial information. *Neurobiology of Learning and Memory*, *91*, 179–185.

Nitz, D. A. (2006). Tracking route progression in the posterior parietal cortex. *Neuron*, *49*, 747–756.

Nitz, D. A. (2012). Spaces within spaces: Rat parietal cortex neurons register position across three reference frames. *Nature Neuroscience*, *15*, 1365–1367.

Nitzan, N., McKenzie, S., Beed, P., English, D. F., Oldani, S., Tukker, J. J., Buzsaki, G., & Schmitz, D. (2020). Propagation of hippocampal ripples to the neocortex by way of a subiculum-retrosplenial pathway. *Nature Communications*, *11*, 1947.

O'Keefe, J. (1976). Place units in the hippocampus of the freely moving rat. *Experimental Neurology*, *51*, 78–109.

O'Keefe, J., & Burgess, N. (1996). Geometric determinants of the place fields of hippocampal neurons. *Nature*, *381*, 425–428.

O'Keefe, J., & Burgess, N. (2005). Dual phase and rate coding in hippocampal place cells: Theoretical significance and relationship to entorhinal grid cells. *Hippocampus*, *15*, 853–866.

O'Keefe, J., & Dostrovsky, J. (1971). The hippocampus as a spatial map. Preliminary evidence from unit activity in the freely-moving rat. *Brain Research*, *34*, 171–175.

O'Keefe, J., & Recce, M. L. (1993). Phase relationship between hippocampal place units and the EEG theta rhythm. *Hippocampus*, *3*, 317–330.

Olshausen, B. A., & Field, D. J. (1996). Natural image statistics and efficient coding. *Network*, *7*, 333–339.

Olshausen, B. A., & Field, D. J. (2004). Sparse coding of sensory inputs. *Current Opinion in Neurobiology*, *14*, 481–487.

Olson, J. M., Li, J. K., Montgomery, S. E., & Nitz, D. A. (2020). Secondary motor cortex transforms spatial information into planned action during navigation. *Current Biology*, *30*(1845–1854), e1844.

Orr, G., Rao, G., Houston, F. P., McNaughton, B. L., & Barnes, C. A. (2001). Hippocampal synaptic plasticity is modulated by theta rhythm in the fascia dentata of adult and aged freely behaving rats. *Hippocampus*, *11*, 647–654.

Packard, M. G., & McGaugh, J. L. (1996). Inactivation of hippocampus or caudate nucleus with lidocaine differentially affects expression of place and response learning. *Neurobiology of Learning and Memory*, *65*, 65–72.

Pastoll, H., Ramsden, H. L., & Nolan, M. F. (2012). Intrinsic electrophysiological properties of entorhinal cortex stellate cells and their contribution to grid cell firing fields. *Frontiers in Neural Circuits*, *6*, 17.

Pavlides, C., Greenstein, Y. J., Grudman, M., & Winson, J. (1988). Long-term potentiation in the dentate gyrus is induced preferentially on the positive phase of theta-rhythm. *Brain Research*, *439*, 383–387.

Pérez-Escobar, J. A., Kornienko, O., Latuske, P., Kohler, L., & Allen, K. (2016). Visual landmarks sharpen grid cell metric and confer context specificity to neurons of the medial entorhinal cortex. *eLife*, *5*, e16937.

Poirazi, P., Brannon, T., & Mel, B. W. (2003). Arithmetic of subthreshold synaptic summation in a model CA1 pyramidal cell. *Neuron*, *37*, 977–987.

Pouget, A., & Sejnowski, T. J. (1997). Spatial transformations in the parietal cortex using basis functions. *Journal of Cognitive Neuroscience*, *9*, 222–237.

Pouget, A., & Snyder, L. H. (2000). Computational approaches to sensorimotor transformations. *Nature Neuroscience*, *3*, 1192–1198.

Poulter, S., Lee, S. A., Dachtler, J., Willis, T. J., & Lever, C. (2021). Vector trace cells in the subiculum of the hippocampal formation. *Nature Neuroscience*, *24*, 266–275.

Poulter, S. L., Lee, S. A., Dachtler, J., Wills, T. J., & Lever, C. (2019). *Vector trace cells in the subiculum of the hippocampal formation*. BioRXiv.

Powell, A., Connelly, W. M., Vasalauskaite, A., Nelson, A. J. D., Vann, S. D., Aggleton, J. P., Sengpiel, F., & Ranson, A. (2020). Stable encoding of visual cues in the mouse Retrosplenial cortex. *Cerebral Cortex*, *30*, 4424–4437.

Qasim, S. E., Fried, I., & Jacobs, J. (2021). Phase precession in the human hippocampus and entorhinal cortex. *Cell*, *184*(3242–3255), e3210.

Quirk, G. J., Muller, R. U., & Kubie, J. L. (1990). The firing of hippocampal place cells in the dark depends on the rat's recent experience. *The Journal of Neuroscience*, *10*, 2008–2017.

Rao, R. P., & Ballard, D. H. (1999). Predictive coding in the visual cortex: A functional interpretation of some extra-classical receptive-field effects. *Nature Neuroscience*, *2*, 79–87.

Rasmussen, D., & Eliasmith, C. (2014). A spiking neural model applied to the study of human performance and cognitive decline on Raven's advanced progressive matrices. *Intelligence*, *42*, 53–82.

Raudies, F., & Hasselmo, M. E. (2015). Differences in visual-spatial input may underlie different compression properties of firing Fields for grid cell modules in medial entorhinal cortex. *PLoS Computational Biology*, *11*, e1004596.

Raudies, F., & Hasselmo, M. E. (2017). A model of symbolic processing in Raven's progessive matrices. *Biologically Inspired Cognitive Architectures*, *21*, 47–58.

Raven, J. (2000). The Raven's progressive matrices: Change and stability over culture and time. *Cognitive Psychology*, *41*, 1–48.

Recce, M., & Harris, K. D. (1996). Memory for places: A navigational model in support of Marr's theory of hippocampal function. *Hippocampus*, *6*, 735–748.

Redish, A. D., & Touretzky, D. S. (1998). The role of the hippocampus in solving the Morris water maze. *Neural Computation*, *10*, 73–111.

Rizzolatti, G., & Fabbri-Destro, M. (2008). The mirror system and its role in social cognition. *Current Opinion in Neurobiology*, *18*, 179–184.

Rizzuto, D. S., Madsen, J. R., Bromfield, E. B., Schulze-Bonhage, A., & Kahana, M. J. (2006). Human neocortical oscillations exhibit theta phase differences between encoding and retrieval. *NeuroImage*, *31*, 1352–1358.

Robertson, R. G., Rolls, E. T., & Georges-Franois, P. (1998). Spatial view cells in the primate hippocampus: Effects of removal of view details. *Journal of Neurophysiology*, *79*, 1145–1156.

Robinson, J., Manseau, F., Ducharme, G., Amilhon, B., Vigneault, E., El Mestikawy, S., & Williams, S. (2016). Optogenetic activation of septal glutamatergic neurons drive hippocampal theta rhythms. *The Journal of Neuroscience*, *36*, 3016–3023.

Robinson, J. C., Brandon, M. P., & Hasselmo, M. E. (2021). Examining the role of medial septal cell types in entorhinal grid cell generation. *Society for Neurosciences*, *P866*, 8.

Rolls, E. T., & O'Mara, S. M. (1995). View-responsive neurons in the primate hippocampal complex. *Hippocampus*, *5*, 409–424.

Rolls, E. T., Robertson, R. G., & Georges-Francois, P. (1997). Spatial view cells in the primate hippocampus. *The European Journal of Neuroscience*, *9*, 1789–1794.

Rolls, E. T., Stringer, S. M., & Elliot, T. (2006). Entorhinal cortex grid cells can map to hippocampal place cells by competitive learning. *Network*, *17*, 447–465.

Rolls, E. T., Treves, A., Robertson, R. G., Georges-Francois, P., & Panzeri, S. (1998). Information about spatial view in an ensemble of primate hippocampal cells. *Journal of Neurophysiology*, *79*, 1797–1813.

Rueckemann, J. W., Sosa, M., Giocomo, L. M., & Buffalo, E. A. (2021). The grid code for ordered experience. *Nature Reviews. Neuroscience*, *22*, 637–649.

Salinas, E., & Abbott, L. F. (1996). A model of multiplicative neural responses in parietal cortex. *Proceedings of the National Academy of Sciences of the United States of America*, *93*, 11956–11961.

Salinas, E., & Abbott, L. F. (1997). Invariant visual responses from attentional gain fields. *Journal of Neurophysiology*, *77*, 3267–3272.

Salinas, E., & Abbott, L. F. (2001). Coordinate transformations in the visual system: How to generate gain fields and what to compute with them. *Progress in Brain Research*, *130*, 175–190.

Samsonovich, A., & McNaughton, B. L. (1997). Path integration and cognitive mapping in a continuous attractor neural network model. *The Journal of Neuroscience*, *17*, 5900–5920.

Sargolini, F., Fyhn, M., Hafting, T., McNaughton, B. L., Witter, M. P., Moser, M. B., & Moser, E. I. (2006). Conjunctive representation of position, direction, and velocity in entorhinal cortex. *Science*, *312*, 758–762.

Savelli, F., Luck, J. D., & Knierim, J. J. (2017). Framing of grid cells within and beyond navigation boundaries. *eLife*, *6*, e21354.

Savelli, F., Yoganarasimha, D., & Knierim, J. J. (2008). Influence of boundary removal on the spatial representations of the medial entorhinal cortex. *Hippocampus*, *18*, 1270–1282.

Schmidt, R., Diba, K., Leibold, C., Schmitz, D., Buzsaki, G., & Kempter, R. (2009). Single-trial phase precession in the hippocampus. *The Journal of Neuroscience*, *29*, 13232–13241.

Schmidt-Hieber, C., & Hausser, M. (2013). Cellular mechanisms of spatial navigation in the medial entorhinal cortex. *Nature Neuroscience*, *16*, 325–331.

Serafin, M., Williams, S., Khateb, A., Fort, P., & Mühlethaler, M. (1996). Rhythmic firing of medial septum non-cholinergic neurons. *Neuroscience*, *75*, 671–675.

Shapiro, M. L., & Hetherington, P. A. (1993). A simple network model simulates hippocampal place fields: Parametric analyses and physiological predictions. *Behavioral Neuroscience*, *107*, 34–50.

Shay, C. F., Boardman, I. S., James, N. M., & Hasselmo, M. E. (2012). Voltage dependence of subthreshold resonance frequency in layer II of medial entorhinal cortex. *Hippocampus*, *22*, 1733–1749.

Shay, C. F., Ferrante, M., Chapman, G. W. T., & Hasselmo, M. E. (2016). Rebound spiking in layer II medial entorhinal cortex stellate cells: Possible mechanism of grid cell function. *Neurobiology of Learning and Memory*, *129*, 83–98.

Sherrill, K. R., Chrastil, E. R., Ross, R. S., Erdem, U. M., Hasselmo, M. E., & Stern, C. E. (2015). Functional connections between optic flow areas and navigationally responsive brain regions during goal-directed navigation. *NeuroImage*, *118*, 386–396.

Sherrill, K. R., Erdem, U. M., Ross, R. S., Brown, T. I., Hasselmo, M. E., & Stern, C. E. (2013). Hippocampus and retrosplenial cortex combine path integration signals for successful navigation. *The Journal of Neuroscience: The Official Journal of the Society for Neuroscience*, *33*, 19304–19313.

Shute, C. C., & Lewis, P. R. (1967). The ascending cholinergic reticular system: Neocortical, olfactory and subcortical projections. *Brain*, *90*, 497–520.

Si, B., Kropff, E., & Treves, A. (2012). Grid alignment in entorhinal cortex. *Biological Cybernetics*, *106*, 483–506.

Sidman, M., Stoddard, L. T., & Mohr, J. P. (1968). Some determinants of visual neglect. *Journal of Neurology, Neurosurgery, and Psychiatry*, *32*, 580–587.

Siegle, J. H., & Wilson, M. A. (2014). Enhancement of encoding and retrieval functions through theta phase-specific manipulation of hippocampus. *eLife*, *3*, e03061.

Skaggs, W. E., McNaughton, B. L., Wilson, M. A., & Barnes, C. A. (1996). Theta phase precession in hippocampal neuronal populations and the compression of temporal sequences. *Hippocampus*, *6*, 149–172.

Solstad, T., Boccara, C. N., Kropff, E., Moser, M. B., & Moser, E. I. (2008). Representation of geometric borders in the entorhinal cortex. *Science*, *322*, 1865–1868.

Solstad, T., Moser, E. I., & Einevoll, G. T. (2006). From grid cells to place cells: A mathematical model. *Hippocampus*, *16*, 1026–1031.

Sotty, F., Danik, M., Manseau, F., Laplante, F., Quirion, R., & Williams, S. (2003). Distinct electrophysiological properties of glutamatergic, cholinergic and GABAergic rat septohippocampal neurons: Novel implications for hippocampal rhythmicity. *The Journal of Physiology*, *551*, 927–943.

Stangl, M., Topalovic, U., Inman, C. S., Hiller, S., Villaroman, D., Aghajan, Z. M., Christov-Moore, L., Hasulak, N. R., Rao, V. R., Halpern, C. H., Eliashiv, D., Fried, I., & Suthana, N. (2021). Boundary-anchored neural mechanisms of location-encoding for self and others. *Nature*, *589*, 420–425.

Stensola, H., Stensola, T., Solstad, T., Froland, K., Moser, M. B., & Moser, E. I. (2012). The entorhinal grid map is discretized. *Nature*, *492*, 72–78.

Stern, C. E., Corkin, S., Gonzalez, R. G., Guimaraes, A. R., Baker, J. R., Jennings, P. J., Carr, C. A., Sugiura, R. M., Vedantham, V., & Rosen, B. R. (1996). The hippocampal formation participates in novel picture encoding: Evidence from functional magnetic resonance imaging. *Proceedings of the National Academy of Sciences of the United States of America*, *93*, 8660–8665.

Stewart, S., Jeewajee, A., Wills, T. J., Burgess, N., & Lever, C. (2014). Boundary coding in the rat subiculum. *Philosophical Transactions of the Royal Society of London. Series B, Biological Sciences*, *369*, 20120514.

Terrazas, A., Krause, M., Lipa, P., Gothard, K. M., Barnes, C. A., & McNaughton, B. L. (2005). Self-motion and the hippocampal spatial metric. *The Journal of Neuroscience*, *25*, 8085–8096.

van Wijngaarden, J. B., Babl, S. S., & Ito, H. T. (2020). Entorhinal-retrosplenial circuits for allocentric-egocentric transformation of boundary coding. *eLife*, *9*, e59816.

Voigts, J., & Harnett, M. T. (2020). Somatic and dendritic encoding of spatial variables in Retrosplenial cortex differs during 2D navigation. *Neuron*, *105*(237–245), e234.

Wainger, B. J., DeGennaro, M., Santoro, B., Siegelbaum, S. A., & Tibbs, G. R. (2001). Molecular mechanism of cAMP modulation of HCN pacemaker channels. *Nature*, *411*, 805–810.

Wang, C., Chen, X., & Knierim, J. J. (2020). Egocentric and allocentric representations of space in the rodent brain. *Current Opinion in Neurobiology*, *60*, 12–20.

Wang, C., Chen, X., Lee, H., Deshmukh, S. S., Yoganarasimha, D., Savelli, F., & Knierim, J. J. (2018). Egocentric coding of external items in the lateral entorhinal cortex. *Science*, *362*, 945–949.

Wang, J., Chen, S., Nolan, M. F., & Siegelbaum, S. A. (2002). Activity-dependent regulation of HCN pacemaker channels by cyclic AMP: Signaling through dynamic allosteric coupling. *Neuron*, *36*, 451–461.

Watrous, A. J., Fried, I., & Ekstrom, A. D. (2011). Behavioral correlates of human hippocampal delta and theta oscillations during navigation. *Journal of Neurophysiology*, *105*, 1747–1755.

Watrous, A. J., Lee, D. J., Izadi, A., Gurkoff, G. G., Shahlaie, K., & Ekstrom, A. D. (2013). A comparative study of human and rat hippocampal low-frequency oscillations during spatial navigation. *Hippocampus*, *23*, 656–661.

Wells, C. E., Amos, D. P., Jeewajee, A., Douchamps, V., Rodgers, J., O'Keefe, J., Burgess, N., & Lever, C. (2013). Novelty and anxiolytic drugs dissociate two components of hippocampal theta in behaving rats. *The Journal of Neuroscience*, *33*, 8650–8667.

Whitlock, J. R., Pfuhl, G., Dagslott, N., Moser, M.-B., & Moser, E. I. (2012). Functional split between parietal and entorhinal cortices in the rat. *Neuron*, *73*, 789–802.

Whitlock, J. R., Sutherland, R. J., Witter, M. P., Moser, M. B., & Moser, E. I. (2008). Navigating from hippocampus to parietal cortex. *Proceedings of the National Academy of Sciences of the United States of America*, *105*, 14755–14762.

Wiener, S. I., Paul, C. A., & Eichenbaum, H. (1989). Spatial and behavioral correlates of hippocampal neuronal activity. *The Journal of Neuroscience*, *9*, 2737–2763.

Wilber, A. A., Clark, B. J., Forster, T. C., Tatsuno, M., & McNaughton, B. L. (2014). Interaction of egocentric and world-centered reference frames in the rat posterior parietal cortex. *The Journal of Neuroscience*, *34*, 5431–5446.

Williams, J. M., & Givens, B. (2003). Stimulation-induced reset of hippocampal theta in the freely performing rat. *Hippocampus*, *13*, 109–116.

Wills, T. J., Barry, C., & Cacucci, F. (2012). The abrupt development of adult-like grid cell firing in the medial entorhinal cortex. *Frontiers in Neural Circuits*, *6*, 21.

Winter, S. S., Clark, B. J., & Taube, J. S. (2015). Disruption of the head direction cell network impairs the parahippocampal grid cell signal. *Science*, *347*, 870–874.

Wirth, S., Baraduc, P., Plante, A., Pinede, S., & Duhamel, J. R. (2017). Gaze-informed, task-situated representation of space in primate hippocampus during virtual navigation. *PLoS Biology*, *15*, e2001045.

Wood, E. R., Dudchenko, P. A., Robitsek, R. J., & Eichenbaum, H. (2000). Hippocampal neurons encode information about different types of memory episodes occurring in the same location. *Neuron*, *27*, 623–633.

Zilli, E. A., & Hasselmo, M. E. (2010). Coupled noisy spiking neurons as velocity-controlled oscillators in a model of grid cell spatial firing. *The Journal of Neuroscience*, *30*, 13850–13860.

Zilli, E. A., Yoshida, M., Tahvildari, B., Giocomo, L. M., & Hasselmo, M. E. (2009). Evaluation of the oscillatory interference model of grid cell firing through analysis and measured period variance of some biological oscillators. *PLoS Computational Biology*, *5*, e1000573.

Zugaro, M. B., Monconduit, L., & Buzsaki, G. (2005). Spike phase precession persists after transient intrahippocampal perturbation. *Nature Neuroscience*, *8*, 67–71.

How to cite this article: Alexander, A. S., Robinson, J. C., Stern, C. E., & Hasselmo, M. E. (2023). Gated transformations from egocentric to allocentric reference frames involving retrosplenial cortex, entorhinal cortex, and hippocampus. *Hippocampus*, *33*(5), 465–487. https://doi.org/10.1002/hipo.23513